Soft Comput (2009) 13:883–904
DOI 10.1007/s00500-008-0351-7

FOCUS

Performance evaluation of memetic approaches in 3D reconstruction of forensic objects

J. Santamaría · O. Cordón · S. Damas · J. M. García-Torres · A. Quirin

Published online: 30 July 2008

Abstract Different tasks in forensics require the use of 3D models of forensic objects (skulls, bones, corpses, etc.) captured by 3D range scanners. Since a whole object cannot be completely scanned in a single image using a range scanner, multiple acquisitions from different views are needed to supply the information to construct the 3D model by a range image registration method. There is an increasing interest in adopting evolutionary algorithms as the optimization technique for image registration methods. However, the image registration community tends to separate global and local searches in two different stages, named sequential hybridization approach, which is opposite to the scheme adopted by the memetic framework. In this work, we aim to analyze the capabilities of memetic algorithms (Moscato in On evolution, search, optimization, genetic algorithms and martial arts: towards memeticalgorithms. Report 826, Caltech Concurrent Computation Program, Pasadena, 1989) for tackling a really complex and challenging real-world problem as the 3D reconstruction of forensic objects. Our intention is threefold: firstly, designing new memetic-based methods for tackling a real-world problem and subsequently carrying out a performance and behavioral analysis of the results; secondly, comparing their performance with the one achieved by other methods based on the classical sequential hybridization approach; and thirdly, concluding the experimental study by highlighting the outcomes achieved by the best method in tackling the real-world problem. Several real-world 3D reconstruction problems from the Physical Anthropology Lab at the University of Granada, Spain, were used to support the evaluation study.

This work was partially supported by the Spain's Ministerio de Educación y Ciencia (ref. TIN2006-00829) and by the Andalusian Dpto. de Innovación, Ciencia y Empresa (ref. TIC1619), both including EDRF fundings.

J. Santamaría
Department of Computer Science,
University of Jaen, Jaen, Spain
e-mail: jslopez@ujaen.es

O. Cordón (✉) · S. Damas · A. Quirin
European Centre for Soft Computing,
Mieres, Asturias, Spain
e-mail: oscar.cordon@softcomputing.es

S. Damas
e-mail: sergio.damas@softcomputing.es

A. Quirin
e-mail: arnaud.quirin@softcomputing.es

J. M. García-Torres
Soft Computing Research Group,
University of Granada, Granada, Spain
e-mail: jmgt@correo.ugr.es

1 Introduction

Image registration (IR) (Zitová B and Flusser 2003) is a fundamental task in image analysis. The aim is to find a correspondence (or transformation) among two or more images taken under different conditions -at different times, using different sensors, from different viewpoints, or a combination of them. In particular, range IR refers to an IR problem where the input images were acquired by a particular device named range scanner.

On the other hand, evolutionary computation (EC) (Bäck et al. 1997) uses computational models of evolutionary processes as key elements in the design and implementation of computer-based problem solving systems. There is an increasing interest on applying EC principles to solve the IR problem (Cordón 2007). Despite the straightforward approaches that usually tackle the problem by means of a genetic algorithm (GA), the *sequential hybridization* bet-

ween global and local strategies is becoming the current trend in the community (Dru et al. 2006; Jenkinson and Smith 2001; Telenczuk et al. 2006; Xu and Dony 2004; Yao and Goh 2006). In this sequential hybridization approach, a global search is first carried out taking advantage of the global search capability of evolutionary algorithms (EAs). Then, some kind of local search algorithm is used for fine tuning the result, usually as a separate stage. This scheme of hybridization is opposite to that considered by the memetic approach where the local search component is embedded in the global search procedure (Ishibuchi et al. 2003; Krasnogor and Smith 2005).

Surprisingly, to the best of our knowledge, we found only one contribution to the problem (Cordón et al. 2006a). In our opinions, memetic algorithms could be a more interesting alternative in view of the knowledge acquired in the evolutionary computation community (Ishibuchi et al. 2003; Ong et al. 2006; Tang et al. 2007; Zhou et al. 2007; Zhu et al. 2007). Hence, we aim to make an advance in the solving of a really complex and challenging real-world problem as the 3D reconstruction of forensic objects, by considering the application of memetic algorithms. Our main goals are threefold. Firstly, we aim to design new memetic-based methods tackling our real-world problem and subsequently carrying out a performance and behavioral analysis of the results reported by them. Secondly, we intend to compare their performance with that of those methods based on the classical sequential hybridization approach. Finally, we also aim to conclude the experimental study by highlighting the outcomes achieved by the best method tackling our real-world problem.

On the other hand, it has been shown in the *No Free Lunch* theorem (Wolpert and Macready 1996) that there is no general method that is able to achieve the best results for all possible problems. Hence, the method used should ideally be tuned for our particular real-world problem at hand. In order to address our three previously marked goals, we have designed nine memetic algorithms [resulting from the combination of three basic EAs: CHC (Eshelman 1991), Differential Evolution (Storn 1997), and Scatter Search (Glover 1977) and three local search techniques: Powell's (1964), Solis and Wets (1981), and Crossover-based local search (XLS) (Beyer and Deb 2001) methods], each with three different intensification degrees as well as two different application criteria of the local search (deterministic vs. probabilistic). The resulting fifty four memetic designs will be compared to the three basic evolutionary approaches (without any local search intensification procedure) and to the nine sequential hybridizations resulting from their combination with the three selected local optimizers. As such, we are considering sixty six different IR methods in our performance study, that will be run on eight real-world skull 3D model reconstruction problem instances. The conclusions of this experimental study will be validated by a statistical test that will properly support the conclusions drawn. As an interesting issue, we should notice that the application considered has a stringent run time requirement, what makes it specially interesting for a study like the one we develop.

This paper is organized as follows. First, Sect. 2 briefly describes the advantages of the range IR approach for the 3D modeling of forensic objects. This section also presents both the mathematical formulation of the range IR problem and the most important contributions following the sequential hybridization approach. Then, Sect. 3 introduces the problem formulation to describe the memetic algorithms considered. The experimental study is included in Sect. 4. Finally, Sect. 5 presents some conclusions from our study and future works.

2 Range image registration and forensic identification

This section is devoted to introduce the basics of the real-world application in forensic identification we are facing. The relation between this application and the generic IR procedure is also presented.

2.1 3D reconstruction of forensic objects by means of range image registration

Range scanners are devices that acquire multiple 3D images of a physical object (views), each one partially recovering the complete geometry of the sensed object and being in a different coordinate system (Fig. 1). Then, in order to build a complete virtual model, there is a need to consider a technique to perform the accurate integration of the different views (Ikeuchi and Sato 2001). The more accurate the alignment of the views, the better the reconstruction of the object. This framework is usually called *range image registration* (RIR), being a particular application of the more generic IR field (see next section) to the specific problem of 3D reconstruction.

On the other hand, some range scanners are provided with a turn table device (Fig. 2) that is connected to the scanner to accurately control the amount of rotation between consecutive acquisitions. Notice that, regardless the existence of the turn table, there are some scenarios where it is useless. That is the case when the size of the object to be scanned or when there is an interest on scanning an excavation, for instance.

Forensic experts need to achieve accurate models of forensic objects (skulls, bones, corpses, etc.) for many different tasks. As an example, we are involved in the *photographic supra-projection* process (Iscan 1993), which is a forensic technique that aims to identify a missing person from the skeletal remains found (especially, the skull) and a photograph of the possible "candidate" composed of the following stages: firstly, the 3D model reconstruction of the skull; secondly, the superimposition of the antemortem photo and

Fig. 1 From left to right. First row corresponds to two range images of the Cleopatra's bust taken by a range scanner from two different points of view. Second row depicts the alignment achieved and the photo of the bust taken with a conventional CCD digital camera

Fig. 2 Arrangement of forensic objects on a Konica–Minolta© turn table

the reconstructed 3D model; and third, the final judgement of the experts based on the study of the existing matching between the landmarks established in both skull model and photograph of the face. Therefore, the confidence of the final identification decision, among other factors, will be based on the accuracy of the reconstructed 3D model of the skull. We have been granted with two different research projects by the Spain's Ministerio de Educación y Ciencia (ref. TIN2006-00829) and by the Andalucia's Dpto. de Innovación, Ciencia y Empresa (ref. TIC1619). The aim is to design an automatic, soft computing-based based procedures to assist the forensic expert in the whole identification process. The contribution in Santamaría et al. (2007) as well as the current one correspond to our recent outcomes regarding the described first stage, while Ballerini et al. (2007) is our first approach to the second one.

2.2 Mathematical formulation

IR is the task that aims to find the optimal point/surface correspondence/overlapping between two (or more) images, captured in a local coordinate system by a specific acquisition procedure, i.e., from different points of views (multiple views), at different times, or by different sensors (Zitová B and Flusser 2003). Such images could be 2D or 3D, depending on the problem tackled. Thus, the key idea of the IR process is to achieve the geometric transformation (rotation, translation, etc.), noted as f, that places different images in a common coordinate system, bringing the points as close together as possible by minimizing the error of a given metric of resemblance, known as similarity metric in the IR literature.

As depicted in Fig. 1, the 3D reconstruction procedure carries out several pair-wise alignments (registrations) of adjacent views, known as scene and model, in order to obtain the final (reconstructed) 3D model of the physical object. Then, every pair-wise RIR method tries to find the Euclidean motion that brings the *scene* view $I_s = \{p_i\}_1^{N_{I_s}}$ into the best possible alignment with the *model* view $I_m = \{q_i\}_1^{N_{I_m}}$, with p_i and q_i being the characteristic points from every image. We have considered an Euclidean motion based on a 3D rigid transformation (f) determined by seven real-coded parameters, that is: a rotation[1] $R = (\theta,\ Axis_x, Axis_y, Axis_z)$ and a translation $\mathbf{t} = (t_x, t_y, t_z)$, with θ and **Axis** being the angle and axis of rotation, respectively. Then, the transformed points of the *Scene* view are denoted by

$$f(p_i) = R(p_i - C_{I_s}) + C_{I_s} + t, \quad f(I_s) = \{f(p_i)\}_1^{N_{I_s}} \quad (1)$$

where C_{I_s} is the center of mass of I_s. We define the distance from a transformed I_s point $f(p_i)$ to the *Model* view I_m as the squared Euclidean distance to the closest point q_{cl} of I_m, $d_i^2 = \|f(p_i) - q_{cl}\|^2$.

Then, the RIR task can be formulated as an optimization problem searching for the Euclidean transformation f^* achieving the best overlapping of both images according to

[1] We used quaternions instead of the three classical Euler matrices representation that suffers the problem of *gimbal lock* (Shoemake 1985).

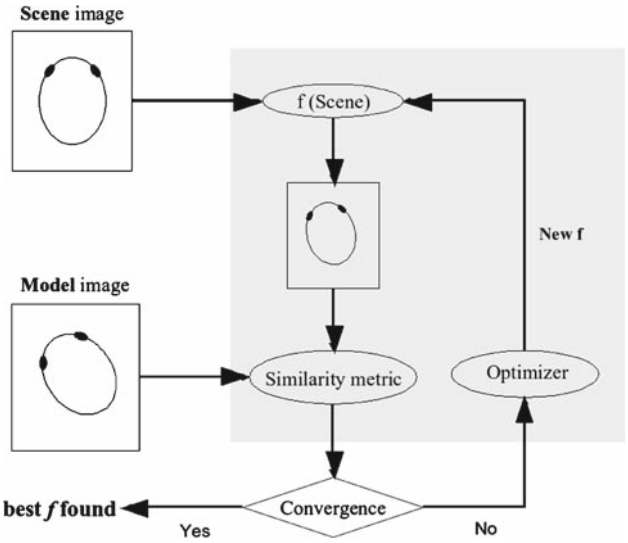

Fig. 3 Flowchart of the optimization process considered in our pairwise RIR framework

the considered *Similarity metric* F:

$$F(I_s, I_m; f) = d_i^2, \forall i \in \{1, \ldots, N_{I_s}\} \quad (2)$$

$$f^* = \arg\min_f F(I_s, I_m; f) \quad s.t.: \; f^*(I_s) \cong I_m \quad (3)$$

Such a transformation estimation is interpreted into an iterative optimization process as shown in Fig. 3.

On the other hand, the successful performance of any RIR method drastically depends on the amount of overlapping present in the couple of range images (likewise, on the number of views acquired). Since our intention is to ease the acquisition procedure to the forensic experts, we have only considered those scanning cases with a minimum overlapping degree, close to the fifty percent of the physical surface. Thus, the number of images taken and stored is reduced. Despite trying to make the acquisition process easier for the forensic experts, notice that the problem complexity is much higher. We know in advance that there will be a large number of points in the scene view I_s that will never correspond to any other in the adjacent model view I_m.

Taking into account the said overlapping consideration, an objective function based on the minimization of the median squared error (MedSE) of the closest point distances d_i^2 is considered:[2]

$$F(I_s, I_m; f) = MedSE(d_i^2) \quad (4)$$

where $MedSE()$ corresponds to the computation of the median d_i^2 value of the $N_{I_s}^{th}$ scene points. We have used the Grid Closest Point (GCP) scheme (Yamany et al. 1999) to speed up the computation of the closest point q_{cl} of I_m.

[2] Notice that we will not use the objective function of our previous contribution (Yamany et al. 1999), to follow a more robust approach.

2.3 Sequential hybridization-based image registration approach

In the last decade, there is an increasing interest in applying EC principles to solve the IR problem (Cordón 2007). This is a great motivation since the classical IR methods of the state of the art [for instance, the ICP algorithm (Besl and McKay 1992)] are not able to escape from local optima solutions mainly originated by the image acquisition procedure. The first preliminary attempts to solve IR using EC can be found in 1984. Such an approach was based on a GA and it was applied to register angiographic 2D images (Fitzpatrick et al. 1984). Since this initial contribution, different authors solved the problem adopting the EC framework but with several important problem formulation and EC design restrictions in their approaches (Cordón 2007). In order to outperform the latter ones, in recent proposals (Cordón et al. 2006a,b), we have introduced different EAs (*CHC and Scatter Search*) with more suitable components to the current EC framework. These contributions allowed us to tackle more complex problems regarding both the extension of the geometric transformation by considering a uniform scaling factor and stronger misalignments between the input images.

Recently, there is a clear tendency in the IR community toward the application of a *sequential hybridization* approach which separately combines global and local search procedures. While the formers are usually based on EC procedures, the latter are mainly based on gradient descent algorithms. In this approach, a global search is first carried out taking advantage of the global search capability of EAs. Then, some kind of local search algorithm is used for fine tuning the previous result. Several instances of that framework are reviewed as follows.

Jenkinson and Smith (2001) faced the affine registration problem of 3D medical image brains. The proposed IR method combines a fast local optimization based on the Powell's method (Press et al. 1999) with an initial full search phase which is conducted over the rotation angles considering a 8-mm cubed voxels (coarse) resolution of the image volumes. The local optimization stage is carried out for upper volumetric resolutions in order to achieve more accurate results.

Xu and Dony (2004) propose an IR method based on the Differential Evolution EA for the global search stage and the Powell's method facing the 3D medical IR problem of 3D magnetic resonance images (MRIs).

Similarly, Telenczuk et al. (2006) used the latter EA-based global search algorithm (Differential Evolution) and the Regular Step Gradient Descent algorithm for fine tuning to face the problem of determining the position of high-resolution molecular structures in medium-resolution macromolecular complexes.

On the other hand, Yao and Goh (2006) faced the 2D IR problem of multisensor images using GAs to obtain a good (coarse) initial registration. It is followed by a fast refining stage using the Powell's method.

Finally, Dru et al. (2006) propose the use of the DIRECT (Dividing Rectangles) deterministic global optimization algorithm and the Powell's method applied to the 3D IR problem of MRIs of human brains.

3 Memetic algorithms for 3D reconstruction

In Sect. 3.1, we first present the recent and short relationship between MAs and the IR problem. Then, Sect. 3.2 introduces the different memetic designs we propose to tackle the RIR problem.

3.1 Image registration and memetic algorithms

The state of the art IR proposals do not usually follow a memetic approach, except for our contribution (Cordón et al. 2006a) which make use of the Scatter Search algorithm. Instead, they use to consider a pure global search design taking advantage of the exploratory capabilities of EC. Nevertheless, as stated in Sect. 2.3, nowadays there is a clear tendency in the IR community toward the application of a *sequential hybridization* approach, being an EA framework opposite to the memetic one where the local search component is embedded in the global search procedure (Ishibuchi et al. 2003; Krasnogor and Smith 2005).

The term memetic algorithm (MA) was introduced by Moscato in 1989 to describe GAs where local search (LS) played a significant role (Moscato 1989). Such a scheme of "hybrid" EA originated because the recombination and mutation operations of GAs usually produce solutions outside the space of local minima (known as global search behavior). Meanwhile, a local optimizer acts to "repair" such solutions and produces new ones that lie within this subspace (local search behavior). Opposite to the sequential hybridization approach, the local search strategy is part of the evolutionary procedure. From that original contribution, the EC community has shown a great interest on MAs resulting in a broad research area (Ishibuchi et al. 2003; Krasnogor and Smith 2005; Ong et al. 2006; Tang et al. 2007; Zhou et al. 2007; Zhu et al. 2007).

We think that the memetic framework could be a more interesting alternative for the IR community. We aim to study if, as expected, memetic approaches can outperform the current IR methods based on the sequential hybridization approach when facing a challenging real-world application, in particular, the 3D reconstruction of forensic objects. The next section presents the new memetic designs from the viewpoint of their use for RIR.

3.2 Considered memetic approaches

Next sections are devoted to introduce the different designs of MAs we have considered for tackling our RIR problem.

3.2.1 Global search strategy

We aim to design MAs that have recently reported successful results tackling the IR problem (Cordón et al. 2006a,b; Salomon et al. 2001). Thus, in the next subsections we describe three of the most outstanding EA approaches to the IR problem: CHC, Differential Evolution, and Scatter Search.

3.2.1.1 ***CHC*** (Eshelman 1991) is a binary-coded EA that involves the combination of a selection strategy with a very high selective pressure, and several components inducing a strong diversity. Its four main components are:

- *An initial generation of solutions:* the initial population of solutions is randomly generated and considered to be evolved.
- *An elitist selection:* the members of the current population are merged with the new population obtained and the best individuals are selected to compose the new population. If a parent and a trial solution has the same objective value, the former is preferred to the latter.
- *A highly disruptive crossover:* HUX crossover guarantees that the two trial solutions are always at the maximum binary Hamming distance from their two parents, thus proposing the introduction of a high diversity in the new population and reducing the tendency of premature convergence.
- *An incest prevention mechanism:* during the reproduction step, each member of the parent (current) population is randomly chosen without replacement and paired for mating. However, not all these couples are allowed to cross over. Before mating, the Hamming distance between the potential parents is calculated and if half this distance does not exceed a fixed difference threshold, they are not allowed to mate and no trial solution coming from them is included in the population. If no trial solution is obtained in one generation, the difference threshold is decremented by one. Therefore, only the most diverse potential parents are mated. However, the required diversity automatically decreases as the population naturally converges.

Besides, CHC is characterized by a restart mechanism to encourage the achievement of a suitable and fast ratio of convergence. This restart is triggered when the difference threshold drops to zero and is applied by maintaining the best solution found so far and randomly generating the remain-

ing of solutions in the new population for evolution until the algorithm reaches the time limit.

In our first approach to the IR problem by adopting EAs (Cordón et al. 2006b), we extended the above CHC scheme to deal with real-coded solutions while keeping its basis as much as possible. Real-coded CHC is also based on the four main components of the original CHC proposal (Eshelman 1993). The initial generation of solutions and the elitist selection are exactly the same. However, there is a need to to use a different real-coded crossover operator. BLX-α (Eshelman 1993), commonly used in real-coded GAs, was considered. This mechanism for combination obtains a trial solution $x = (h_1, \ldots, h_k, \ldots, h_l)$ (with l being the number of parameters of the rigid transformation and h_k a given value for such k^{th} variable) from the two parent solutions $x^1 = (c_1^1, \ldots, c_l^1)$ and $x^2 = (c_1^2, \ldots, c_l^2)$ by uniformly generating a random value for each variable h_k in the interval $[c_{min} - I \cdot \alpha\ ,\ c_{max} + I \cdot \alpha]$, with $c_{max} = \max(c_k^1, c_k^2)$, $c_{min} = \min(c_k^1, c_k^2)$, and $I = c_{max} - c_{min}$. Hence, the parameter α allows us to make this crossover as disruptive as desired enabling a more appropriate trade-off between exploration and exploitation. Finally, there is also a need to adapt the original CHC incest prevention mechanism (whose operation is guided by the Hamming distance). We considered a binary conversion of the parent solutions to be combined in order to be able to measure the similarity between them. The difference threshold is then proportionally set up imitating the original CHC algorithm.

3.2.1.2 ***Differential evolution (DE)*** was introduced by Storn (1997). It is a parallel direct search method based on EAs that has proved to be a promising candidate to solve real valued optimization problems. DE combines simple arithmetic operators with the classical crossover, mutation and selection operators within an easy to implement scheme and with few control parameters. Indeed, these advantages could influence the recent publication of several contributions that use the DE scheme for tackling the IR problem (De Falco et al. 2008; Salomon et al. 2001; Telenczuk et al. 2006; Xu and Dony 2004). The reported results showed a competitive performance against traditional approaches and they also achieved a fast ratio of convergence.

The fundamental idea of DE is a new scheme for generating trial solutions by adding the weighted differenced vector between two population members to a third one. There is a number of DE variants to be utilized (Price 1999). After a preliminary experimentation, we considered the DE/Random/1/Exp version which is summarized in the following steps:

Population initialization: initialize a random population of solutions according to a uniform probability distribution.

Mutation or differential operation: first, for each $x_i(t)$ solution of the population at generation t, a differential vector z_i is generated according to Eq. (5)

$$z_i = x_{r_1}(t) + F \cdot [x_{r_2}(t) - x_{r_3}(t)] \tag{5}$$

where i is the solution's population index at generation t; r_1, r_2, r_3 are three randomly generated integers (for each i^{th} solution) with uniform distribution and their values are lower than or equal to the population size, and mutually different; and F is the *mutation factor* ($F > 0$) which controls the amplification of the difference between two individuals.

Recombination operation: next, in order to increase the diversity of the new trial solution $x_i(t+1)$ to be generated, recombination is applied by replacing certain parameters (randomly selected with uniform distribution according to the *recombination rate* $CR \in [0, 1]$) of the $x_i(t)$ solution by the corresponding parameters of the previously generated differential vector z_i as follows:
For each j^{th} *parameter of* $x_i(t)$
If $Rand(j) \leq CR$ *then* $x_{i_j}(t+1) = z_{i_j}$
Otherwise, $x_{i_j}(t+1) = x_{i_j}(t)$

Selection operation: if the new trial solution $x_i(t+1)$ is better than the compared one $x_i(t)$, then the later will be replaced by the former.

A restart mechanism is also considered to avoid the search stagnation. In this case, a certain number of iterations without inserting any new individual in the population is usually the criterion to apply such a mechanism. The new initial population is generated as it was done for CHC.

3.2.1.3 ***Scatter search (SS)*** (Glover 1977) is a really novel EA instance since it violates the premise that these algorithms must be based on randomization (although it is also compatible with randomized implementations). SS fundamentals were originally proposed by Glover and have been later developed in some texts (Laguna and Martí 2003). The main idea of this technique is based on a *systematic* combination of solutions (instead of a randomized one like that usually done in GAs) taken from a considerably reduced evolved pool of solutions named *Reference set* (between five and ten times lower than usual GA population sizes). This way, an efficient and accurate search process is encouraged thanks to the latter and to innovative components comprising the algorithm (see Fig. 4).

The fact that the mechanisms within SS are not restricted to a single uniform design allows the exploration of strategic possibilities that may prove effective in our particular study. Of the five methods in the SS methodology, only four are strictly required. The *Improvement Method*, which plays a clear local search role, is usually needed if high quality outcomes are desired. However, an SS procedure can be implemented without it. Hence, to clearly differentiate between the memetic and the sequential hybridization SS-based

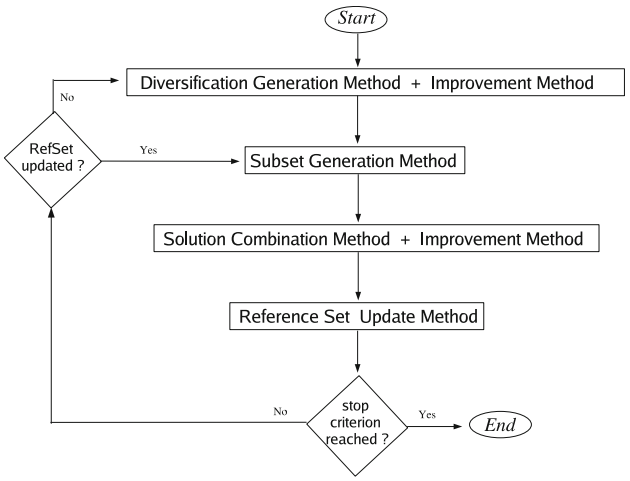

Fig. 4 The control diagram of SS

approaches, we will consider the *Improvement Method* only for the memetic SS designs.

Next, we introduce the five SS methods and their specific design considered in our previous contribution (Santamaría et al. (2007)) for tackling the RIR problem.

Diversification generation method: the original template of the SS algorithm considers the generation of an initial collection of *diverse* trial solutions to build the Reference set. The number of generated solutions is usually five or ten times greater than the *Reference set* size (noted $Psize$). Notice that these trial solutions are not randomly (as usually happens with GAs) but heuristically generated. However, we have considered a randomized generation of the initial solutions for a fair comparison with the previous EAs (CHC and DE) in Sect. 4. In the memetic versions, we do not apply the *Improvement method* to these initial diverse solutions either, as the original SS proposal suggested, for the sake of fair comparison.

Improvement method: this method plays a clear local search or intensification role by transforming a trial solution into one (or more) enhanced trial solution. If no improvement occurs, the input solution is considered as a result. As said, this is an optional method in the SS design allowing us to consider different SS approaches to the RIR problem: a memetic one (where the improvement method is included) or a sequential hybridization one (where the intensification is postponed as a final stage). While we used the *Solis&Wets'* algorithm in Santamaría et al. (2007), in this contribution we consider the said *Powell's, Solis & Wets', and Crossover-based LS (XLS)* methods for the different memetic SS designs, as well as for the intensification stage of the sequential hybridizations (see Sect. 3.2.2).

Reference set update method: it builds and maintains a small Reference set consisting of the b (e.g., no more than 20) best solutions found, according to their quality (objective function value) or their diversity (distance between solutions). In this case, we considered an updating criterion based on the quality of solutions, and a static scheme.

Subset generation method: from the solutions in the Reference set, it typically produces a subset of couples of solutions as a basis for creating combined solutions. We take into account all the $(\frac{b\cdot(b-1)}{2})$ possible pairs of solutions present in the *Reference set*.

Solution combination method: this method transforms a given set of solutions (typically, a couple) into one new combined solution. We chose the BLX-α crossover operator for this method.

Similar to the global search EAs presented, a restart mechanism is considered to avoid local minima. In this case, the same one considered for DE is applied.

3.2.2 Local search strategy

In the next subsections, we will describe the LS methods that we have selected to design the MA-based RIR approaches. Note that there is no analytic expression of the objective function in our real-world problem. Thus, none of the following LS methods require any differentiation of the objective function. This is an advantage because every design of MA in this work could be easily used in any other problem with similar features.

3.2.2.1 ***Powell's method*** (Powell 1964) is one of the most popular optimization algorithms in the IR literature (Dru et al. 2006; Maes et al. 1999; Xu and Dony 2004; Zhu and Cochoff 2002). It is classified as a *direction-set* optimization algorithm, which is one that seeks to calculate an optimal basis for the space of the objective function such that the unit vectors are well suited to 1D optimization. That is, an optimal choice of basis vectors should provide step descent, while satisfying the following criterion: optimization along one-dimension minimally disturbs previously computed optimizations along other basis dimensions. Thus, Powell's algorithm works by repeatedly performing successive 1D optimizations along a set of basis vectors. The orientation of the set of basis vectors is revised to increase the rate of descent. Our implementation is based on Brent's method for one-dimensional optimization (Press et al. 1999).

3.2.2.2 ***Solis & Wets' method*** (Solis and Wets 1981) is a stochastic direct search algorithm (based on a greedy local search heuristic) that has extensively been used for continuous optimization. It generates trial points using a multi-

variate normal distribution, and unsuccessful trial points are reflected about the current point to find (as in the hill climbing scheme) a descent direction.

In particular, the algorithm generates new trial solutions using coordinate-wise steps. If the obtained solution is better than the current best one then it is accepted and the algorithm is repeated. Otherwise, the algorithm considers a step in the opposite direction. If this new point is also worse than the current best solution then a new trial solution is again generated in the neighborhood of the current one. The method also defines mechanisms for expanding and contracting the step size of the offsets used to generate the new trial solutions.

3.2.2.3 ***Crossover-based LS (XLS) methods*** (Beyer and Deb 2001) are a singular class of optimization methods that are especially attractive for real-coding problems. Indeed, they consider crossover operators that have a self-adaptive nature. Such operators can generate trial solutions adaptively according to the distribution of the parents solutions in the population without any adaptive parameters. The most usual examples of XLS methods are *Minimal Generation Gap* (Satoh and Kobayashi 1996) and *Generalized Generation Gap* (Deb and Joshi 2002).

The fundamental idea of XLS is to induce an LS on the neighborhood of the parents solutions involved in crossover (Lozano et al. 2004; Noman and Iba 2005). Given a solution to be improved, called family father, L solutions are randomly selected in the current population for mating with the previous one to generate new trial solutions in the father's neighborhood by performing crossover operations. Finally, a selection operation is carried out for replacing the family father with the best solution of the L new solutions only if this one is better than the former. Hence, it can be called *best point neighborhood strategy* (Noman and Iba 2005). This procedure is repeated until the considered stop criterion is reached.

In this work, we considered the PBX-α crossover operator (Lozano et al. 2004) (with $\alpha = 0.5$) to generate four neighbor solutions every LS iteration.

3.2.3 Global and local search integration

Embedding LS as an operator in an EA can better deal with the rate of convergence and/or the accuracy requirements of the particular problem to be tackled, hence striking a balance between global and local searches is mandatory (Ishibuchi et al. 2003; Tang et al. 2007; Zhu et al. 2007). Both issues are of crucial importance in our real-world application. Furthermore, this component plays a key role inside the MA framework and several design decisions should be taken into account for a proper behavior.

LS is usually applied to each trial solution obtained from crossover/mutation operations in each iteration of the EA (Costa et al. 1995; Merz and Freisleben 1999). However, it is very time-consuming, especially in applications where the objective function takes a long time like ours. Hence, it could be a risky decision if accuracy is not the only requirement but reduced run time is also a need. This is why alternative approaches consider the application to only one solution, the best one found in the current population; or to any other taken by a proper selection criterion (Ishibuchi et al. 2003; Herrera et al. 2005; Noman and Iba 2005).

Another chance is to consider a selective application of the LS on every individual, that is the one we will take in this work. Then, the question is: which is the considered criterion to either apply LS or not to a solution? This decision will affect important factors in the stochastic optimization framework such as the suitable trade-off between intensification and diversification.

In our real application, we think that applying LS to every trial solution could excessively decrease the exploratory capabilities of the global search strategies of these MAs. Indeed, as stated in (Krasnogor and Smith 2005), "The majority of MAs in the literature apply local search to every individual in every generation of the evolutionary algorithm, our model makes it clear that this is not mandatory." Hence, we have considered two different LS selective application criteria. They both are easy to implement and we have recently obtained promising results tackling the IR problem using them in Cordón et al. (2008) and Cordón et al. (2006a), respectively. The first criterion was originally proposed by Hart (1994) and later used in some contributions such as Krasnogor and Smith (2000) and Lozano et al. (2004). It is based on a random application with uniform distribution considering a probability value of 0.0625. On the other hand, the second criterion considers a deterministic scheme: the trial solution will be improved using the LS method only if it is better than any of its parents. Both LS application criteria will be compared in the experimental study developed in Sect. 4.

Finally, since we are dealing with a real application, we have a speed requirement that forces us to consider a prefixed time (in seconds) for each method in our study. Given such fixed period of time as stopping criterion, one final issue that could significantly affect the diversification–intensification trade-off is the number of LS iterations we are considering, i.e., the higher the number of LS iterations, the higher the intensification (and the lower the diversification) our algorithm is applying. We will consider three different number of LS iterations to study the influence of this parameter: 25, 50, and 100 evaluations.

4 Computational study

In this section we aim to study the performance and the behavior of the different designed RIR methods to automati-

Table 1 Size of the range images of the considered datasets in their original conditions and after the feature extraction process

		Views/images				
		270°	315°	0°	45°	90°
Original	$Skull_1$	109936	76794	68751	91590	104441
	$Skull_2$	121605	116617	98139	118388	128163
Crest lines	$Skull_1$	1380	1181	986	1322	1363
	$Skull_2$	1528	2106	1995	2066	1774

cally generate 3D models of skulls with a minimal intervention of the forensic experts. As mentioned in Sect. 2.1, this reconstruction stage is the first step of the whole photographic supra-projection process. It plays a crucial role because the more accurate the reconstructed skull model is, the more reliable the identification decision will be.

4.1 Skull image datasets

The Physical Anthropology Lab at the University of Granada, Spain, provided us with two datasets of human skulls[3] acquired by a Konica–Minolta© 3D Lasserscanner VI-910. It should be hightlighted that the couple of forensic objects considered for this experimental study were chosen by the experts according to several forensic criteria to guarantee a maximal differentiation regarding to skull features.

To ease the forensics' work, we have taken into account important factors regarding to the scanning process like time and storage demand. Indeed, we consider a scan every 45° of the turn table.[4] Hence, we deal with a sequence of only eight different views: $0° - 45° - 90° - 135° - 180° - 225° - 270° - 315°$, which supposes a great reduction both in the scanning time and storage requirements. The datasets we will use in our experiments are limited to five of the eight views: $270° - 315° - 0° - 45° - 90°$. The reason is that our aim is to achieve a 3D model of the most interesting parts of the skull for the final objective of our research project, the craniofacial identification of a missing person, i.e., the frontal part of the skull.

We will consider a feature-based IR approach which aims to reduce the huge datasets IR algorithms must typically deal with, by selecting a small set of truly representative characteristics. We use a preprocessing algorithm that carries out the extraction of feature points from the range images by applying a 3D crest lines edge detector (Yoshizawa et al. 2005). Thus the resulting datasets will be the ones used by every RIR method. Table 1 summarizes the size (number of image points) of the forensic range images of the considered skulls before and after the application of the crest line extraction procedure. Figure 5 shows some of the skulls range images and their corresponding extracted feature points.

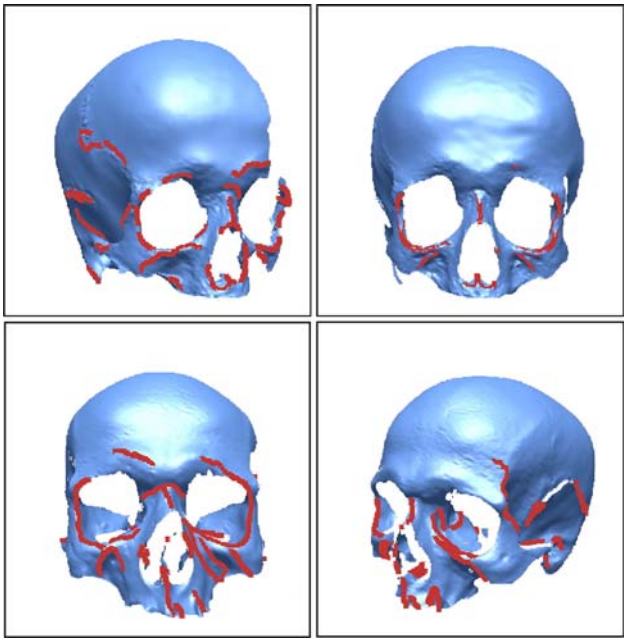

Fig. 5 From left to right. First row corresponds to images $I^1_{315°}$ and $I^1_{0°}$ of $Skull_1$. Second row collects images $I^2_{0°}$ and $I^2_{45°}$ of $Skull_2$. Each of the four images comprises both the original skull (in *light gray*/*blue*) and the crest line dataset (in *dark grey*/*red*)

4.2 Experimental design

We will focus our attention on the design of automatic, accurate, robust, and fast RIR methods based on MAs, comparing their performance with those proposals existing in the IR literature adopting a sequential hybridization approach.

On the one hand, the experimental design addresses eight different pair-wise RIR problems: the first four regarding to $Skull_1$: $I^1_{270°} - I^1_{315°}$, $I^1_{315°} - I^1_{0°}$, $I^1_{45°} - I^1_{0°}$, and $I^1_{90°} - I^1_{45°}$; and the remainder corresponding to $Skull_2$: $I^2_{270°} - I^2_{315°}$, $I^2_{315°} - I^2_{0°}$, $I^2_{45°} - I^2_{0°}$, and $I^2_{90°} - I^2_{45°}$.

[3] We can not provide these datasets as public domain due to the spanish law for protection of personal data.

[4] Notice that the lesser the overlapping between pairs of images (when prominent rotation angle of the turn table is considered), the more chances for the classical RIR methods, as the so called ICP algorithm (Besl and McKay 1992), to get stuck in local optima (Santamaría et al. 2007).

On the other hand, it is based on those ill-conditioned situations where forensics are advocated to manually intervene to reconstruct an optimal skull 3D model. That is the aim of the following RIR problem instances. They simulate an unsupervised scanning process where there is no turn table available or the particular environment does not allow its use. Specifically, the RIR instances are designed from a rigid transformation (see Sect. 2.2), noted T_i, which is applied to one of the two images of every pair-wise RIR problem. For instance, $T_i(I^2_{45^\circ}) - I^2_{0^\circ}$ represents a certain RIR instance to be tackled by every RIR method, where the rigid transformation T_i is applied to the $I^2_{45^\circ}$ image to be placed in some other location different from its correct original one. RIR methods aim to recover the original dataset location (the inverse transformation T_i^{-1}) achieving a minimum distance (or maximum overlapping) criterion between the couple of images.

We will consider different rigid transformations T_i in every run of the considered RIR methods. Each of these transformations will simulate a typical bad situation for the forensics in which, for instance, there is no positional device or the object could suffer any displacement not been controlled by them. Indeed, such transformations (see Sect. 2.2) will be randomly generated with a uniform distribution as follows: each of the three rotation axis parameters will be in the range $[-1, 1]$; the rotation angle will be in $[0°, 360°]$; and the three translation parameters in $[-40, 40]$. This search space significantly influences (negatively, of course) the performance of classical RIR methods (Santamaría et al. 2007; Zhang 1994), which usually deal with a transformation that slightly modifies the object location. Thus, any of the RIR methods considered in this work will have to overcome such really bad initializations to be considered an automatic, accurate, robust, and quick reconstruction method of forensic objects.

4.3 Parameter settings

The different RIR methods have been run on a 2.2 GHz. AMD ATHLON processor with 2 GB RAM and the GNU/Linux SuSe 10.1 (32 bits) O.S. using the GNU/gcc compiler without code optimization. Considering the speed requirement of our real-world application, both the MAs and the basic EA stage of the sequential hybridization approaches are run for the same fixed time of 20 s. It is worth noting that in order to avoid execution dependence, every RIR method will tackle thirty different runs for each of the eight considered RIR problem instances. Since we consider 20 s for each of the four subproblems comprising a skull reconstruction, we will be able to provide a skull 3D model in just 80 s, which is a great improvement from the forensic expert point of view.

The three MA-based RIR methods (built from CHC, DE, and SS) start from a population of 100 random solutions. The value of the parameter α of the BLX-α operator employed in CHC is set to 0.5 (Cordón et al. 2006b). On the other hand, the best configuration we found for the control parameters of the DE-based MA takes a mutation factor $F = 0.5$ and a recombination rate $CR = 0.7$. In the SS-based MA, the RefSet is composed of $b = 8$ solutions and the BLX-α crossover operator is applied with $\alpha = 0.3$ (Santamaría et al. 2007).

The LS step of the sequential hybridization-based RIR methods (applied once the previous EA stage is finished) considers a stop criterion based on a predefined number of evaluations without improvement. In particular, we consider $4 \cdot$*number-of-parameters-of-solutions=28*. Notice that this final refinement step is not taken into account in the 20 seconds run time since it spends a very short amount of time. Even so, sequential hybridizations are slightly benefited from this consideration.

Finally, the restart mechanism is applied for DE and SS when the same population is kept during three iterations.

4.4 Analysis of results

This section is devoted to analyze the results following the three main goals we initially defined. The notation we consider for every RIR method is as follows:

$$Approach^{EA}_{LS/sel\_criterion/\#it}$$

where $Approach$ takes one value in $\{MA, SH\}$, according to the memetic or the sequential hybridization approach, EA corresponds to one of the three considered EAs $\{CHC, DE, SS\}$, LS is either $\{Powell, Solis, XLS\}$, $sel\_criterion \in \{d, p\}$ to respectively differentiate between a deterministic and a probabilistic LS application criterion, and $\#it \in \{25, 50, 100\}$ corresponds to the LS intensification level. For instance, $MA^{DE}_{Solis/d/25}$ refers to a MA which considers DE as its EA and the Solis&Wets method as its LS, which uses a deterministic criterion for the LS application and an intensity level of 25 evaluations each time LS is considered for application. On the other hand, SH^{DE}_{Solis} corresponds to a sequential hybridization RIR method using DE for global search and the Solis&Wets LS method as the refinement step.

By considering all these designs and parameter values combinations, we will be able to analyze their influence on different aspects of the problem solving performance, for instance the intensification/diversification trade-off according to the $\#it$ of the LS, the LS application criteria, the LS method, and the EA scheme considered.

For the sake of understanding, the statistical results we present in Sects. 4.4.1–4.4.3 correspond to the overall averaged objective function [see Eq. (4)] obtained by averaging the MedSE values of the eight RIR problem instances for every RIR method (basic EA, sequential hybridization, or MA-based). In the Appendix, Tables 8, 9, 10 and 11 show the detailed results of the eight considered RIR instances. Notice that every particular RIR problem has been tackled performing 30 different runs to avoid execution dependence

Table 2 Statistical results (the overall averaged MedSE and, between brackets, the standard deviation values) for the three basic EAs and the three sequential hybridization-based RIR methods

	Basic EA	Sequential hybridizations		
		Powell	Solis	XLS
CHC	30.75 (19.36)	30.20 (18.22)	30.68 (18.16)	**30.17** (18.46)
DE	41.62 (19.74)	**35.56** (18.29)	40.88 (18.47)	39.03 (18.22)
SS	31.45 (19.66)	**31.38** (18.44)	31.45 (18.39)	31.45 (18.39)

Bold values remark the sequential hybridization-based RIR method with the best performance

of the results. On the other hand, the said MedSE is a distance value related to the range scanner resolution and it specifically represents squared millimeters. Thus, the more accurate the reconstructed skull model is, the lower this value will be.

Finally, the Mann–Whitney U test, also known as Wilcoxon ranksum test, has been used for a deeper statistical study of the results. Unlike the commonly used t test, the Wilcoxon test does not assume normality of the samples, which would be unrealistic for the data of our real-world application (Lehmann 1975). The significance tables presented in the next sections are comprised by three symbols:'+' means the significance is favorable to the method in the row; '−' stands for the significance favorable to the method in the column; and '=' is used when there is not significance favorable (not relevant) to any of the couple of methods being compared.

4.4.1 Sequential hybridization-based RIR methods

Table 2 presents the aggregated results of the basic EA and the sequential hybridization-based RIR methods and Fig. 6 summarizes them according to the overall averaged MedSE value (Table 8 in the Appendix shows the individual results of the eight considered RIR instances). Table 3 shows the statistical significance (considering a 5% significance level) of the results obtained by the considered methods.

4.4.1.1 Technical analysis: Compared to the basic DE-based RIR method which performs a more exploratory search, the other two considering CHC and SS perform a more effective search thanks to their better trade-off between diversification and intensification. In relation to the latter, notice that the three SH^{DE} RIR methods achieve a more important improvement over the basic DE version than the one obtained by SH^{CHC} and SH^{SS} over their basic CHC and SS versions, respectively.

According to the considered fine tuning (i.e., local search) algorithms, the Powell's method provides more chances for improvement when the sequential hybridization approach is considered, as it is also reported in recent contributions of the state of the art (Dru et al. 2006; Jenkinson and Smith 2001; Telenczuk et al. 2006; Xu and Dony 2004; Yao and Goh 2006). Despite being computationally more expensive than the Solis & Wets and the XLS algorithms, we noticed how the Powell's method offers a better performance when the starting solution provided by the first EA stage is near the basin of attraction of the optimum. In particular, we highlight the good properties of such algorithm in the SH^{DE}_{Powell} RIR method, which achieves an improvement of a 14.6%.

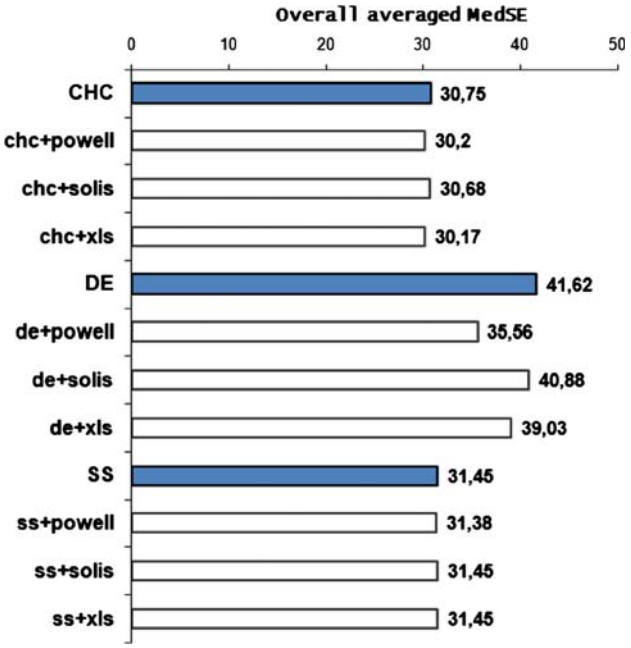

Fig. 6 Basic EA and sequential hybridization RIR methods with the best overall averaged MedSE results

4.4.1.2 Performance comparison: The first row in Table 3 shows how the performance of the three families of sequential hybridizations is usually significantly better than that of the simple EAs. In particular, the third row of this table reveals how $SH^{CHC}_{Powell}/SH^{CHC}_{XLS}$, SH^{DE}_{Powell}, and SH^{SS}_{Powell} are the sequential hybridization RIR methods achieving the best results, respectively, in each case.

Finally, in Table 4 we show the statistical significance regarding the best sequential hybridization RIR methods. Entries with an additional symbol means that it has been

Table 3 Statistical significance (considering a 5% significance level) of the obtained results by the basic EAs and the sequential hybridization RIR methods

	CHC					DE					SS			
	CHC	SH^{CHC}_{XLS}	SH^{CHC}_{Powell}	SH^{CHC}_{Solis}		DE	SH^{DE}_{XLS}	SH^{DE}_{Powell}	SH^{DE}_{Solis}		SS	SH^{SS}_{XLS}	SH^{SS}_{Powell}	SH^{SS}_{Solis}
CHC	•	−	−	=	DE	•	−	−	−	SS	•	=	−	=
SH^{CHC}_{XLS}	+	•	=	+	SH^{DE}_{XLS}	+	•	−	+	SH^{SS}_{XLS}	=	•	−	=
SH^{CHC}_{Powell}	+	=	•	+	SH^{DE}_{Powell}	+	+	•	+	SH^{SS}_{Powell}	+	+	•	+
SH^{CHC}_{Solis}	=	−	−	•	SH^{DE}_{Solis}	+	−	−	•	SH^{SS}_{Solis}	=	=	−	•

Table 4 Statistical significance (considering a 5% and a 10% significance level) regarding the best sequential hybridization RIR methods

		SH^{CHC}_{Powell}	SH^{DE}_{Powell}	SH^{SS}_{Powell}
SH^{CHC}_{Powell}	**(30.20)**	•	=,+	=
SH^{DE}_{Powell}	(35.56)	=,−	•	−
SH^{SS}_{Powell}	(31.38)	=	+	•

found a significance value considering a 10% significance level. From that table and Fig. 6 we can draw the following conclusions:

- SH^{CHC}_{Powell} is the algorithm with the best average value.
- The difference between SH^{CHC}_{Powell} and SH^{SS}_{Powell} is not significant, which could be due to a bias according to the considered number of runs (supported by the good results also achieved by the Powell's method in both the DE and the SS hybrid algorithms).
- SH^{DE}_{Powell} is the worst sequential hybridization algorithm, considering both the average values and the statistical significance (regardless of how the latter performed considering a 5 or a 10% significance level).

4.4.2 Memetic-based RIR methods

Table 5 presents the averaged statistical results of all the memetic RIR methods regarding the three selected EAs (Tables 9, 10 and 11 in the Appendix show the detailed results of the eight considered RIR instances): CHC, DE, and SS. The statistical significance (considering a 5% significance level) is also included with the corresponding $+, -, =$ symbols to show the favorable, unfavorable or irrelevant significance with respect to the best memetic RIR method (that one with the lowest overall averaged MedSE value among all the methods in its family), highlighted with the • symbol. Likewise, Fig. 7 shows the performance of the six best memetic RIR methods of each of the three families, according to their overall behavior.

4.4.2.1 Technical analysis: A top-down analysis based on the design criteria adopted for the MAs considered is shown as follows:

- *Local search intensification level*: the behavior of the (six) best MA-based RIR methods of every family (see Fig. 7) is different. On the one hand, MA^{CHC} and MA^{SS} families require the lowest intensification level (in all the six cases for the former, in three of the six cases for the latter). On the other hand, the MA^{DE} family require the highest intensification level in three of the six best methods. This is related to the proper exploration/exploitation trade-off induced by the global search considered, i.e., the more exploration the induced global search carries out, the more exploitation is needed in the applied LS. As stated for the sequential hybridization approach, the memetic RIR methods using DE are those incurring greater intensification resources (larger number of iterations) in order to compensate for the high degree of diversification induced in the global search component.
  Contrary to the families of MAs based on DE and SS, all the best MA^{CHC} methods require the lowest LS intensity level (25) to achieve those best results (see Fig. 7). Such configuration is not casual since the CHC algorithm is known to cause a very high selective pressure.
- *Local search application criteria*: Those MAs considering the deterministic criterion improve their probabilistic counterparts in all cases. The deterministic criterion helps to maintain a suitable trade-off between intensification and diversification, due to the considerable reduction of the resources assigned to the LS component, which only considers quality solutions each time it is applied. This issue reveals that a more systematic scheme for the application of LS is more suitable than those mainly based on random decisions in our real-world application.
- *Local search method*: we can rank in descending order of performance (i.e., from the worst to the best result achieved) the (6) methods of each family of MAs: first,

Table 5 Statistical results (overall averaged MedSE and standard deviation values, $\widehat{\mu}$ and $\widehat{\sigma}$, respectively) obtained by the memetic RIR methods based on CHC, DE, and SS

		LS method and intensification level ($\#it$)								
		Powell			Soils			XLS		
		25	50	100	25	50	100	25	50	100
$MA^{CHC}_{*/p/*}$	$\widehat{\mu}$ ($\pm\widehat{\sigma}$)	32.50 (17.10)	37.55 (19.53)	44.23 (16.25)	35.04 (17.06)	37.56 (16.43)	41.32 (21.36)	32.77 (18.35)	34.67 (16.96)	35.32 (18.54)
	Sign.	=	−	−	−	−	−	−	−	−
$MA^{CHC}_{*/d/*}$	$\widehat{\mu}$ ($\pm\widehat{\sigma}$)	30.84 (17.40)	34.29 (18.82)	38.98 (16.54)	30.75 (19.53)	32.97 (18.62)	33.66 (19.14)	**28.91** (17.27)	29.12 (18.48)	29.77 (18.43)
	Sign.	−	−	−	=	−	−	•	=	=
Basic CHC $\widehat{\mu}$ ($\pm\widehat{\sigma}$)	30.75 (19.36)									
Sign.	=									
$MA^{DE}_{*/p/*}$	$\widehat{\mu}$ ($\pm\widehat{\sigma}$)	51.57 (20.59)	62.04 (21.65)	70.02 (25.71)	40.51 (19.98)	40.63 (21.12)	38.17 (20.65)	36.37 (18.38)	35.46 (17.79)	34.89 (18.70)
	Sign.	−	−	−	−	−	−	−	=	−
$MA^{DE}_{*/d/*}$	$\widehat{\mu}$ ($\pm\widehat{\sigma}$)	50.34 (20.49)	59.52 (22.16)	68.64 (25.62)	38.39 (20.30)	38.10 (20.04)	35.63 (21.33)	33.42 (18.19)	34.78 (19.36)	**32.87** (19.33)
	Sign.	−	−	−	−	−	=	=	=	•
Basic DE $\widehat{\mu}$ ($\pm\widehat{\sigma}$)	41.62 (19.74)									
Sign.	−									
$MA^{SS}_{*/p/*}$	$\widehat{\mu}$ ($\pm\widehat{\sigma}$)	42.55 (16.63)	39.38 (20.73)	40.52 (21.77)	26.96 (18.41)	29.46 (17.85)	28.87 (18.82)	29.94 (17.73)	30.22 (17.93)	28.38 (17.36)
	Sign.	−	−	−	=	−	−	−	−	−
$MA^{SS}_{*/d/*}$	$\widehat{\mu}$ ($\pm\widehat{\sigma}$)	36.80 (18.47)	41.70 (19.51)	45.14 (17.42)	26.81 (20.44)	28.45 (18.60)	28.75 (17.38)	25.64 (17.96)	25.63 (17.23)	**25.20** (17.66)
	Sign.	−	−	−	=	−	−	=	=	•
Basic $SS\widehat{\mu}$ ($\pm\widehat{\sigma}$)	31.45 (19.66)									
Sign.	−									

Bold values remark the memetic-based RIR method with the best performance

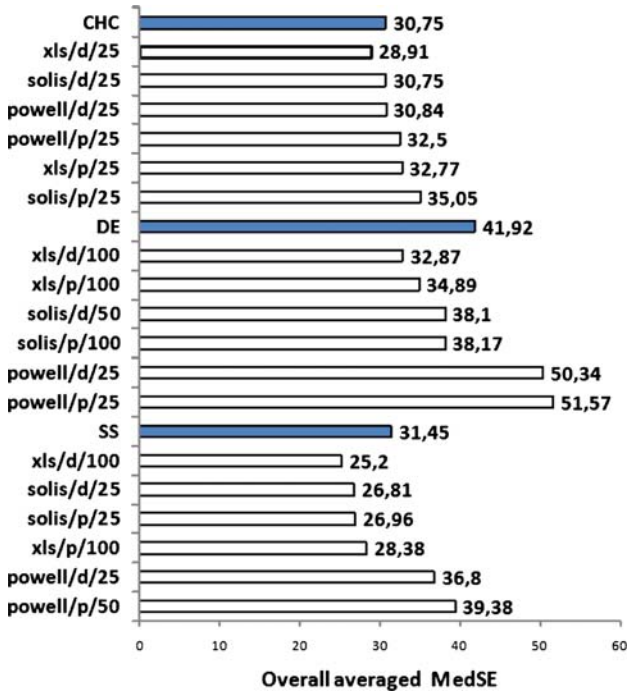

Fig. 7 Basic EA and MA-based RIR methods with the best overall averaged MedSE results

Powell; second, Solis&Wets; and third, XLS. It is remarkable that the Powell's method obtains the worst results for the memetic designs of the MA^{DE} and the MA^{SS} families, especially for the former ones, and only middle quality results for the MA^{CHC} one. That behavior is explained because it leads those methods to a premature convergence. Thus, unlike the sequential hybridization-based RIR methods, Powell's method is not a proper election to achieve a competitive memetic RIR method, regardless of the family of MAs we consider, due to its excessive intensification power.

On the other hand, the Solis&Wets and the XLS methods have a more exploratory behavior due to their stochastic nature. Hence, they provide a better trade-off between the global and local searches. In particular, XLS offers the best results in the majority of the cases. Furthermore, our results encourage the conclusions drawn in (Lozano et al. 2004; Noman and Iba 2005) regarding the benefits of the use of the XLS algorithm.

Finally, we can rank the three families of MAs according to the number of methods outperforming their basic EA counterpart (CHC, DE, or SS). While four of the six RIR methods of both MA^{DE} and MA^{SS} families outperform their basic versions, only one of the RIR methods corresponding to the MA^{CHC} family, $MA^{CHC}_{XLS/d/25}$, improves the results of the RIR method based on the basic CHC. We conclude that this EA itself already provides an appropriate trade-off between intensification and diversification. However, this is not a surprising fact in the MA community. For example, the results obtained by Whitley et al. (2003) were worse than ours and the authors commented on that it was impossible for them to achieve a memetic version able to outperform the basic CHC EA algorithm.

4.4.2.2 Performance comparison: Despite $MA^{CHC}_{XLS/d/25}$ being the only MA^{CHC} method with a lower (better) overall averaged MedSE value than that of its basic CHC version, the statistical significance values included in Table 5 show that this performance difference is not significant, which reinforces the conclusion that CHC is not a good choice to be included in a memetic scheme as mentioned in the previous paragraph. On the other hand, as the significance test demonstrates, each of the best memetic RIR methods of the MA^{DE} and MA^{SS} families outperforms their respective basic EAs.

Finally, Table 6 shows the statistical significance regarding the best memetic RIR methods. From this table, we can deduce that:

- $MA^{SS}_{XLS/d/100}$ is the algorithm with the best average value and it is also significantly better than the other two memetic approaches.
- $MA^{DE}_{XLS/d/100}$ is the algorithm with the worst average value and it is significantly worse than $MA^{CHC}_{XLS/d/25}$.
- Therefore, the ranking of the memetic designs performance is clear: $MA^{SS}_{XLS/d/100}$, $MA^{CHC}_{XLS/d/25}$, and finally $MA^{DE}_{XLS/d/100}$.

4.4.3 Overall performance comparison: sequential hybridization and memetic approaches

Once both families of approaches, i.e., sequential hybridizations and MAs, for tackling our RIR problems have been analyzed indepently, we will go one step forward to compare

Table 6 Statistical significance (considering a 5% significance level) regarding the best memetic RIR methods

		$MA^{CHC}_{XLS/d/25}$	$MA^{DE}_{XLS/d/100}$	$MA^{SS}_{XLS/d/100}$
$MA^{CHC}_{XLS/d/25}$	(28.91)	•	+	−
$MA^{DE}_{XLS/d/100}$	(32.87)	−	•	−
$MA^{SS}_{XLS/d/100}$	**(25.20)**	+	+	•

Table 7 Statistical significance (considering a 5 and a 10% significance level) regarding the best sequential hybridization vs. the best MA-based RIR methods

		SH^{CHC}_{Powell} (30.20)	SH^{DE}_{Powell} (35.56)	SH^{SS}_{Powell} (31.38)
$MA^{CHC}_{XLS/d/25}$	(28.91)	=	+	=
$MA^{DE}_{XLS/d/100}$	(32.87)	=	+	=
$MA^{SS}_{XLS/d/100}$	**(25.20)**	=, +	+	+

their behavior. This study aims to determine which is the most convenient approach, as well as the global best method to face our real-world application: 3D reconstruction of forensic objects (i.e., the second and third goals of this work, respectively).

Table 7 shows the statistical significance regarding the best sequential hybridization vs. the best MA-based RIR methods. Entries with an additional symbol mean that it has been found a significance value considering a 10% significance level. In view of the results contained on it, we can remark the following comments:

- Considering the overall averaged performance, every MA outperforms its sequential hybridization counterpart. However, such difference is only statistically significant for SS and DE, not for CHC.
- MA^{DE}_{XLS} is worse than the two best sequential hybridization algorithms based on CHC and SS. Although these differences are not statistically significant, the latter together with the fact that the DE-based variant of the sequential hybridization is the worst of the three considered. It highlights the weaknesses show of the DE algorithm in solving the problem, regardless the approach.
- Although the second ranked MA, $MA^{CHC}_{XLS/d/25}$, outperforms the two best sequential hybridization approaches based on CHC and SS (and consequently the third one based on DE as well), these differences are not statistically significant. Hence, it seems that, *although MAs usually outperform their sequential hybridization counterparts, a suitable memetic design is needed to properly overcome the performance of the sequential hybridizations* .
- The best overall algorithm to tackle our real-world problem is $MA^{SS}_{XLS/d/100}$, as it achieves the best performance with an averaged value of 25.20 against a 30.20, 35.56, and 31.38 for the best sequential hybridization-based methods (SH^{CHC}_{Powell}, SH^{DE}_{Powell}, and SH^{SS}_{Powell}, respectively) as well as the other two best MA-based methods, $MA^{CHC}_{XLS/d/25}$ and $MA^{DE}_{XLS/d/100}$, achieving values of 28.91 and 32.87, respectively. Regarding the statistical test with a 5% significance level, $MA^{SS}_{XLS/d/100}$ differences are significant with respect to the other two MAs (see Table 6) and the sequential hybridization algorithms based on DE and SS (see Table 7). Moreover, it also significantly outperforms the sequential hybridization of CHC if we consider a 10% significance level.[5] Hence, this particular design of MA achieves the best trade-off between intensification and diversification promoted by the good interaction established between the considered global and local search procedures, i.e., the SS EA and the XLS LS.
- Finally, we can conclude that not every MA outperforms its sequential hybridization counterpart. A proper memetic design is demanded instead, in order to find the proper intensification-diversification trade-off.

4.4.4 3D models of the reconstructed skulls

As said, the best algorithm in our performance study considering both the overall averaged outcomes as well as the statistical significance was $MA^{SS}_{XLS/d/100}$. Since we have a turn table in our scenario (see Sect. 2.1), we are able to know the perfect model of the reconstructed skulls and we can compare it to our 3D reconstructed model. This comparison was performed by the forensic experts of the Physical Anthropology Lab at the University of Granada, Spain, who validated our good results. The first and second rows of Fig. 8 show the best reconstructed 3D models of $Skull_1$ and $Skull_2$ obtained by the $MA^{SS}_{XLS/d/100}$-based RIR (on the left) and the perfect 3D models (on the right). In spite of different colors having been used to easily differentiate among the component 3D views, they perfectly overlap in the reconstructed model after the RIR process. Indeed, there is no visible difference between the reconstructed and the ground truth models in both skulls.

5 Conclusions and future work

In this work, we aimed to improve our initial results tackling a challenging real-world problem from the forensic field considering the *3D reconstruction of forensic objects* (Santamaría et al. 2007). Our intention was threefold:

[5] To properly analyze this result, we should mention that (considering a 5% significance level) the Wilcoxon's distribution, R_+, and R_- values are, respectively, 3, 33, and 3. Since the Wilcoxon's distribution value is not greater than the minimum of R_+ and R_- (actually, it is equal to it) then the condition that rejects the null hypothesis (equality of means) does not hold. However, if we consider a 10% significance level, the Wilcoxon's distribution value becomes 5, what statistically justifies the difference.

Table 8 Statistical results (minimum, mean, and standard deviation) of the 30 runs in each of the eight RIR problems instances (P_1 to P_8) performed by the three basic EAs and the three sequential hybridization-based RIR methods

		Basic CHC	Sequential hybrid CHC		
			Powell	Solis	XLS
P_1	Min	20.01	20.01	20.01	20.01
	μ ($\pm\sigma$)	22.93 (7.52)	22.90 (7.51)	22.93 (7.52)	22.91 (7.51)
P_2	Min	35.89	35.89	35.89	35.89
	μ ($\pm\sigma$)	36.45 (0.47)	36.23 (0.47)	36.45 (0.47)	36.37 (0.46)
P_3	Min	58.69	57.94	58.69	58.69
	μ ($\pm\sigma$)	69.75 (19.02)	69.23 (19.21)	69.75 (19.02)	69.64 (19.06)
P_4	Min	21.05	21.05	21.05	21.05
	μ ($\pm\sigma$)	37.10 (17.98)	36.93 (17.77)	37.10 (17.98)	37.05 (17.92)
P_5	Min	1.98	1.97	1.98	1.98
	μ ($\pm\sigma$)	6.17 (12.96)	5.53 (10.76)	6.17 (12.96)	5.63 (11.00)
P_6	Min	24.25	24.04	24.25	24.25
	μ ($\pm\sigma$)	37.26 (24.56)	36.42 (24.59)	37.26 (24.56)	36.60 (24.55)
P_7	Min	8.79	8.79	8.79	8.79
	μ ($\pm\sigma$)	16.78 (16.95)	14.90 (16.48)	16.24 (15.34)	13.70 (12.85)
P_8	Min	5.55	5.55	5.55	5.55
	μ ($\pm\sigma$)	19.52 (19.36)	19.47 (19.38)	19.52 (19.36)	19.49 (19.36)
$P_1 \cdots P_8$	μ ($\pm\sigma$)	30.75 (19.36)	30.20 (18.22)	30.68 (18.16)	**30.17** (18.46)
		Basic DE	Sequential hybrid DE		
			Powell	Solis	XLS
P_1	Min	20.01	20.01	20.01	20.01
	μ ($\pm\sigma$)	32.07 (20.25)	28.86 (17.93)	31.47 (18.87)	29.73 (18.75)
P_2	Min	35.89	35.89	35.89	35.89
	μ ($\pm\sigma$)	45.10 (21.71)	43.33 (21.24)	44.72 (21.50)	44.44 (21.45)
P_3	Min	59.40	58.09	59.40	59.20
	μ ($\pm\sigma$)	80.83 (24.67)	75.61 (23.64)	80.47 (24.63)	78.61 (25.22)
P_4	Min	21.10	21.10	21.10	21.10
	μ ($\pm\sigma$)	39.21 (20.38)	36.50 (19.36)	39.21 (20.38)	37.49 (20.28)
P_5	Min	2.02	2.02	2.02	2.02
	μ ($\pm\sigma$)	15.47 (14.05)	10.06 (12.00)	14.64 (13.10)	14.19 (13.93)
P_6	Min	24.28	24.25	24.28	24.28
	μ ($\pm\sigma$)	53.69 (22.59)	40.40 (14.48)	51.74 (19.10)	47.30 (22.04)
P_7	Min	9.30	9.10	9.30	9.30
	μ ($\pm\sigma$)	40.72 (26.64)	30.46 (25.41)	39.61 (26.26)	38.34 (26.70)
P_8	Min	5.91	5.86	5.91	5.86
	μ ($\pm\sigma$)	25.83 (22.70)	19.28 (21.32)	25.17 (22.44)	22.14 (21.88)
$P_1 \cdots P_8$	$\widehat{\mu}$ ($\pm\widehat{\sigma}$)	41.62 (19.74)	**35.56** (18.29)	40.88 (18.47)	39.03 (18.22)
P_1	Min	19.76	19.76	19.76	19.76
	μ ($\pm\sigma$)	28.07 (14.13)	28.06 (14.14)	28.07 (14.13)	28.07 (14.13)
P_2	Min	35.89	35.89	35.89	35.89
	μ ($\pm\sigma$)	41.79 (20.68)	41.78 (20.68)	41.79 (20.68)	41.79 (20.68)
P_3	Min	58.10	58.10	58.10	58.10
	μ ($\pm\sigma$)	71.12 (18.28)	71.12 (18.28)	71.12 (18.28)	71.12 (18.28)
P_4	Min	21.10	21.10	21.10	21.10
	μ ($\pm\sigma$)	35.64 (23.25)	35.62 (23.26)	35.64 (23.25)	35.64 (23.25)

Table 8 continued

		Basic SS	Sequential hybrid SS		
			Powell	Solis	XLS
P_5	Min	1.97	1.97	1.97	1.97
	μ ($\pm\sigma$)	9.09 (14.24)	9.09 (14.24)	9.09 (14.24)	9.09 (14.24)
P_6	Min	24.25	24.25	24.25	24.25
	μ ($\pm\sigma$)	33.66 (14.51)	33.66 (14.51)	33.66 (14.51)	33.66 (14.51)
P_7	Min	8.72	8.72	8.72	8.72
	μ ($\pm\sigma$)	12.82 (11.00)	12.81 (11.00)	12.82 (11.00)	12.82 (11.00)
P_8	Min	5.75	5.75	5.75	5.75
	μ ($\pm\sigma$)	19.42 (19.92)	18.91 (20.04)	19.42 (19.92)	19.42 (19.92)
$P_1 \cdots P_8$	$\widehat{\mu}$ ($\pm\widehat{\sigma}$)	31.45 (19.66)	**31.38** (18.44)	31.45 (18.39)	31.45 (18.39)

Bold values remark the sequential hybridization-based RIR method with the best performance

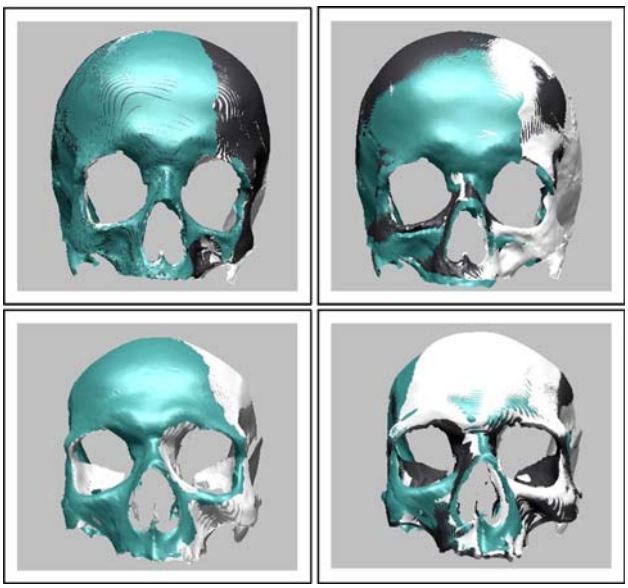

Fig. 8 From left to right. First row, best reconstructed and perfect models of $Skull_1$. Second row, best reconstructed and perfect models of $Skull_2$

- Design new memetic-based methods tackling our real-world problem and subsequently carrying out a performance and behavioral analysis of the results reported by them.
- Compare their performance with the one achieved by other methods based on the classical sequential hybridization approach.
- Highlight the outcomes achieved by the best method tackling our real-world problem.

After a wide performance and behavioral study we can draw some conclusions regarding each of these three main goals:

- Independently the EA considered in the first stage of the sequential hybridization approach, the LS method which offers the best overall results is the Powell's method in comparison with the other two inspired in a more stochastic nature, Solis&Wets and XLS. This behavior reveals that the power of the former approach is based on adopting LS methods with a strong gradient descent component. It also confirms the proper design of the majority of sequential hybridization approaches found in the IR literature. On the other hand, the reverse behavior arises when those LS methods are used in the memetic approach, being the XLS method with the highest intensity level of LS the one providing the best results. Moreover, the former XLS design combined with the use of a deterministic criterion for the application of the LS achieves the best performance. In particular, embedding the latter scheme into the SS EA allows us to obtain a suitable trade-off between intensification and diversification.
- In general, MAs do not always outperform their sequential hybridizations counterparts. In particular, there is only one memetic design of the family of memetic methods based on CHC outperforming the corresponding sequential hybridization. Moreover, that improvement is not significant according to the statistical tests. On the other hand, the memetic designs based on DE and SS are always able to improve the related sequential hybridization methods, although the improvement is not always statistically significant. Therefore, *if we want to find the best algorithm for the problem, it is not enough to replace a sequential hybridization approach by a memetic one, but a good memetic design is also demanded.*
- Finally, the best algorithm for our 3D reconstruction problem was $MA^{SS}_{XLS/d/100}$ considering both the overall averaged outcomes and the statistical significance. This particular MA confirms our previous remark on the importance of a suitable memetic design against the

Table 9 Statistical results (minimun, mean, and standard deviation values) of the 30 (RIR problem instances) runs in each of the eight RIR problems (P_1 to P_8) performed by the CHC-based RIR method and the memetic RIR methods based on CHC

Basic CHC										
		P_1	P_2	P_3	P_4	P_5	P_6	P_7	P_8	$P_1 \cdots P_8$
	Min	20.01	35.89	58.69	21.05	1.98	24.25	8.79	5.55	
	μ ($\pm\sigma$)	22.93 (7.52)	36.45 (0.47)	69.75 (19.02)	37.10 (17.98)	6.17 (12.96)	37.26 (24.56)	16.78 (16.95)	19.52 (19.36)	**30.75** (19.36)
	Sign.								=	

MA based on CHC with a probabilistic application of LS										
		Powell			Solis			XLS		
		25	50	100	25	50	100	25	50	100
P_1	Min	20.01	20.01	20.01	19.83	20.01	20.59	19.87	20.01	20.01
	μ ($\pm\sigma$)	23.75 (8.50)	28.35 (17.37)	33.74 (21.70)	31.43 (18.82)	32.54 (14.41)	32.06 (10.06)	24.86 (11.05)	30.50 (15.35)	27.27 (11.68)
P_2	Min	35.89	35.89	36.26	35.89	35.92	37.61	35.89	35.89	35.89
	μ ($\pm\sigma$)	36.84 (0.57)	41.97 (20.67)	46.09 (19.79)	37.82 (3.03)	44.03 (11.16)	47.37 (7.95)	36.93 (1.66)	39.39 (11.51)	39.43 (4.75)
P_3	Min	58.26	58.66	59.29	59.40	58.66	62.72	58.26	58.26	58.10
	μ ($\pm\sigma$)	72.53 (20.72)	80.96 (22.30)	80.09 (19.68)	74.03 (14.80)	72.29 (15.84)	89.27 (16.58)	75.80 (23.09)	72.74 (17.20)	78.03 (16.84)
P_4	Min	21.10	21.10	21.10	21.10	21.37	22.12	21.10	21.10	21.10
	μ ($\pm\sigma$)	33.04 (15.71)	38.37 (18.20)	41.23 (19.32)	31.69 (15.77)	36.06 (12.53)	38.62 (11.26)	32.23 (16.50)	34.09 (15.80)	34.47 (15.32)
P_5	Min	1.98	1.98	2.02	2.02	2.02	2.21	1.98	2.02	2.05
	μ ($\pm\sigma$)	11.41 (17.52)	11.79 (17.64)	20.46 (18.97)	11.77 (12.03)	15.23 (11.38)	15.25 (12.97)	11.18 (14.52)	11.53 (13.22)	10.96 (11.42)
P_6	Min	24.29	24.38	24.77	24.72	24.77	25.06	24.28	24.25	24.72
	μ ($\pm\sigma$)	35.91 (14.04)	47.92 (21.56)	51.64 (19.91)	40.27 (15.68)	46.02 (16.01)	49.06 (13.73)	38.48 (16.06)	41.01 (12.73)	41.51 (13.06)
P_7	Min	8.79	8.79	9.36	9.03	8.79	9.85	8.79	8.79	9.10
	μ ($\pm\sigma$)	20.63 (20.78)	26.46 (21.04)	45.43 (28.42)	32.36 (20.77)	34.10 (25.37)	39.51 (20.29)	20.47 (17.56)	26.23 (22.03)	28.16 (17.04)
P_8	Min	5.55	5.86	5.86	5.86	5.86	5.91	5.55	5.86	5.86
	μ ($\pm\sigma$)	25.88 (22.90)	24.61 (24.44)	35.20 (24.57)	20.92 (19.76)	20.18 (15.09)	19.44 (12.57)	22.23 (22.05)	21.87 (20.79)	22.71 (17.81)
$P_1 \cdots P_8$	$\widehat{\mu}$ ($\pm\widehat{\sigma}$)	**32.50** (17.10)	37.55 (19.53)	44.23 (16.25)	*35.04* (17.06)	37.56 (16.43)	41.32 (21.36)	*32.77* (18.35)	34.67 (16.96)	35.32 (18.54)
	Sign.	=	−	−	−	−	−	−	−	−

MA based on CHC with a deterministic application of LS										
		Powell			Solis			XLS		
		25	50	100	25	50	100	25	50	100
P_1	Min	20.01	20.01	20.01	20.01	20.01	20.71	20.01	20.01	20.01
	μ ($\pm\sigma$)	27.17 (13.68)	26.13 (13.29)	31.06 (14.04)	23.62 (9.53)	26.75 (10.48)	27.67 (10.12)	24.67 (10.56)	25.39 (11.89)	24.13 (8.83)
P_2	Min	35.89	35.89	36.26	35.89	36.26	37.53	35.89	35.92	35.89
	μ ($\pm\sigma$)	37.03 (0.60)	37.17 (0.99)	39.04 (2.98)	37.38 (1.53)	38.60 (2.01)	40.95 (3.70)	36.91 (0.62)	37.07 (0.96)	37.34 (1.04)
P_3	Min	58.69	58.69	59.75	59.42	61.18	64.97	58.26	58.69	59.20
	μ ($\pm\sigma$)	70.67 (17.62)	76.66 (20.12)	73.98 (18.64)	75.71 (18.14)	75.30 (14.59)	76.31 (9.76)	67.92 (13.98)	71.01 (18.19)	71.74 (14.04)
P_4	Min	21.10	21.10	21.76	21.10	22.12	22.23	21.05	21.10	21.10
	μ ($\pm\sigma$)	30.98 (14.67)	36.08 (17.80)	37.72 (16.11)	32.63 (15.86)	29.97 (10.93)	30.49 (8.86)	26.90 (11.94)	27.87 (12.79)	28.34 (11.46)
P_5	Min	1.98	2.17	2.95	2.05	2.59	2.49	1.97	1.98	2.02
	μ ($\pm\sigma$)	9.34 (15.31)	9.72 (14.01)	14.49 (14.52)	6.76 (6.56)	9.52 (9.77)	9.36 (6.57)	7.46 (10.77)	7.31 (10.82)	6.45 (6.26)
P_6	Min	24.29	25.51	27.01	24.93	25.06	26.06	24.33	24.29	24.72
	μ ($\pm\sigma$)	33.91 (12.51)	42.97 (13.93)	52.30 (15.66)	33.53 (9.09)	39.33 (11.02)	39.93 (9.71)	33.41 (11.53)	33.64 (9.46)	33.96 (7.95)
P_7	Min	8.79	9.13	11.32	9.33	10.45	10.59	8.79	8.79	9.36
	μ ($\pm\sigma$)	22.17 (19.17)	25.73 (18.24)	34.20 (17.77)	22.20 (15.63)	28.41 (14.52)	30.19 (14.62)	19.78 (16.20)	18.54 (13.30)	22.00 (13.16)
P_8	Min	5.86	6.22	7.34	5.86	6.25	6.40	5.55	5.86	5.86
	μ ($\pm\sigma$)	15.48 (17.84)	19.89 (19.99)	29.02 (19.51)	14.18 (14.70)	15.88 (12.02)	14.37 (9.96)	14.24 (16.73)	12.09 (12.56)	14.20 (14.77)
$P_1 \cdots P_8$	$\widehat{\mu}$ ($\pm\widehat{\sigma}$)	*30.84* (17.40)	34.29 (18.82)	38.98 (16.54)	*30.75* (19.53)	32.97 (18.62)	33.66 (19.14)	**28.91** (17.27)	29.12 (18.48)	29.77 (18.43)
	Sign.	−	−	−	=	−	−	•	=	=

Bold values remark the memetic-based RIR method based on CHC with the best performance when considering both the probabilistic and the deterministic application of LS

Table 10 Statistical results (minimun, mean, and standard deviation values) of the 30 (RIR problem instances) runs in each of the 8 RIR problems (P_1 to P_8) performed by the DE-based RIR method and the memetic RIR methods based on DE

Basic DE

		P_1	P_2	P_3	P_4	P_5	P_6	P_7	P_8	$P_1 \cdots P_8$
	min	20.01	35.89	59.40	21.10	2.02	24.28	9.30	5.91	
	μ ($\pm\sigma$)	32.07 (20.25)	45.10 (21.71)	80.83 (24.67)	39.21 (20.38)	15.47 (14.05)	53.69 (22.59)	40.72 (26.64)	25.83 (22.70)	**41.62** (19.74)
	Sign.								–	

MA based on DE with a probabilistic application of LS

		Powell			Solis			XLS		
		25	50	100	25	50	100	25	50	100
P_1	Min	20.16	20.71	20.71	20.61	20.71	20.71	20.01	20.01	20.01
	μ ($\pm\sigma$)	41.11 (23.55)	55.49 (27.66)	56.59 (25.17)	30.92 (10.60)	31.88 (11.85)	29.57 (8.76)	28.77 (12.57)	30.34 (13.04)	26.43 (11.62)
P_2	Min	35.89	37.63	37.63	37.63	37.63	37.63	36.72	36.38	36.26
	μ ($\pm\sigma$)	60.56 (35.15)	79.52 (41.17)	87.69 (46.71)	48.59 (15.50)	48.71 (9.10)	47.10 (6.60)	42.93 (8.13)	40.40 (4.27)	40.90 (5.65)
P_3	Min	60.02	66.86	75.56	64.53	65.50	65.10	59.60	59.42	60.02
	μ ($\pm\sigma$)	94.25 (26.71)	106.02 (26.61)	123.55 (30.84)	83.48 (11.78)	87.07 (16.82)	82.06 (9.89)	74.62 (14.55)	73.69 (14.40)	75.44 (13.24)
P_4	Min	21.49	21.40	22.45	22.27	22.27	22.88	21.10	21.37	21.40
	μ ($\pm\sigma$)	50.04 (20.70)	57.00 (19.17)	59.56 (20.07)	39.47 (13.21)	40.43 (13.69)	37.56 (11.94)	36.08 (14.87)	34.85 (15.08)	34.03 (12.66)
P_5	Min	2.21	2.47	3.53	2.57	2.71	2.96	2.17	2.02	2.17
	μ ($\pm\sigma$)	21.92 (15.82)	31.66 (22.19)	38.29 (23.51)	14.87 (10.22)	13.59 (10.34)	11.71 (7.31)	10.97 (10.50)	10.10 (10.31)	11.88 (10.48)
P_6	Min	25.06	25.89	28.33	25.72	26.66	26.24	25.06	25.13	24.94
	μ ($\pm\sigma$)	61.38 (24.47)	67.26 (25.48)	83.45 (30.31)	51.68 (15.64)	49.10 (15.55)	48.13 (12.94)	47.48 (15.43)	44.64 (16.52)	45.44 (16.07)
P_7	Min	10.71	12.00	16.61	9.55	11.42	9.88	9.50	9.63	9.33
	μ ($\pm\sigma$)	51.82 (24.76)	59.29 (22.92)	65.81 (25.25)	33.49 (16.36)	34.31 (16.48)	33.66 (13.83)	32.63 (20.19)	30.62 (17.39)	29.46 (18.14)
P_8	Min	6.25	6.25	7.38	6.25	6.25	6.25	5.86	6.12	6.12
	μ ($\pm\sigma$)	31.49 (21.66)	40.05 (22.20)	45.22 (19.98)	21.59 (14.56)	19.97 (12.34)	15.54 (8.60)	17.49 (13.59)	19.07 (15.43)	15.57 (12.30)
$P_1 \cdots P_8$	$\widehat{\mu}$ ($\pm\widehat{\sigma}$)	*51.57* (20.59)	62.04 (21.65)	70.02 (25.71)	40.51 (19.98)	40.63 (21.12)	*38.17* (20.65)	36.37 (18.38)	35.46 (17.79)	**34.89** (18.70)
	Sign.	–	–	–	–	–	–	–	=	–

MA based on DE with a deterministic application of LS

		Powell			Solis			XLS		
		25	50	100	25	50	100	25	50	100
P_1	Min	20.71	20.71	23.37	20.01	20.71	20.40	20.01	20.01	20.01
	μ ($\pm\sigma$)	40.08 (21.56)	45.73 (21.66)	59.13 (24.82)	29.91 (9.97)	30.93 (10.54)	27.81 (7.14)	26.96 (11.92)	28.29 (13.07)	23.84 (4.85)
P_2	Min	37.63	37.63	39.52	37.63	37.63	37.63	35.89	36.56	36.66
	μ ($\pm\sigma$)	57.50 (30.21)	67.52 (32.52)	79.25 (35.12)	46.90 (13.20)	46.62 (10.39)	43.35 (4.40)	38.93 (4.21)	39.47 (4.13)	39.56 (4.78)
P_3	Min	61.60	68.14	74.17	64.66	65.72	63.76	59.29	60.36	61.18
	μ ($\pm\sigma$)	89.67 (23.71)	103.99 (25.56)	116.43 (25.82)	82.85 (17.57)	82.25 (13.57)	83.27 (14.52)	74.90 (13.20)	77.69 (18.17)	76.25 (13.31)
P_4	Min	21.95	22.37	27.40	22.12	22.39	22.79	21.13	21.49	21.10
	μ ($\pm\sigma$)	44.99 (19.33)	52.43 (19.57)	64.55 (15.42)	37.37 (12.80)	35.94 (10.32)	34.51 (9.83)	30.68 (12.39)	36.67 (17.49)	31.20 (11.97)
P_5	Min	2.39	3.05	5.13	2.60	2.71	2.50	2.02	2.05	2.02
	μ ($\pm\sigma$)	18.48 (13.94)	28.13 (18.75)	29.07 (16.61)	12.54 (8.98)	12.31 (8.44)	10.31 (7.02)	10.62 (9.21)	10.89 (9.93)	8.41 (8.10)
P_6	Min	26.26	29.77	36.70	25.39	26.24	25.72	24.96	24.72	25.08
	μ ($\pm\sigma$)	67.76 (28.04)	78.43 (30.56)	92.64 (31.68)	46.90 (14.76)	45.99 (13.74)	43.75 (11.68)	40.39 (11.12)	42.60 (13.30)	40.23 (11.27)
P_7	Min	9.77	14.12	12.65	10.71	11.48	11.54	9.45	9.71	9.77
	μ ($\pm\sigma$)	51.37 (21.64)	57.79 (22.38)	63.43 (22.62)	32.13 (16.82)	31.90 (14.92)	28.62 (12.63)	26.69 (14.60)	28.19 (16.87)	27.90 (17.42)
P_8	Min	6.25	7.37	10.65	6.25	6.25	6.39	5.86	5.94	5.94
	μ ($\pm\sigma$)	32.84 (22.67)	42.15 (24.88)	44.60 (20.55)	18.52 (10.66)	18.87 (12.84)	13.42 (6.03)	18.17 (17.14)	14.42 (13.18)	15.55 (13.91)
$P_1 \cdots P_8$	$\widehat{\mu}$ ($\pm\widehat{\sigma}$)	*50.34* (20.49)	59.52 (22.16)	68.64 (25.62)	38.39 (20.30)	38.10 (20.04)	*35.63* (21.33)	33.42 (18.19)	34.78 (19.36)	**32.87** (19.33)
	Sign.	–	–	–	–	–	=	=	=	•

Bold values remark the memetic-based RIR method based on DE with the best performance when considering both the probabilistic and the deterministic appliction of LS

Table 11 Statistical results (minimun, mean, and standard deviation values) of the 30 (RIR problem instances) runs in each of the eight RIR problems (P_1 to P_8) performed by the SS-based RIR method and the memetic RIR methods based on SS

Basic SS

		P_1	P_2	P_3	P_4	P_5	P_6	P_7	P_8	$P_1 \cdots P_8$
	Min	19.76	35.89	58.10	21.10	1.97	24.25	8.72	5.75	
	$\mu(\pm\sigma)$	28.07 (14.13)	41.79 (20.68)	71.12 (18.28)	35.64 (23.25)	9.09 (14.24)	33.66 (14.51)	12.82 (11.00)	19.42 (19.92)	**31.45** (19.66)
	Sign.								–	

MA based on SS with a probabilistic application of LS

		Powell			Solis			XLS		
		25	50	100	25	50	100	25	50	100
P_1	Min	35.89	19.76	19.59	20.01	19.59	20.01	19.43	19.43	19.76
	μ ($\pm\sigma$)	45.80 (28.52)	29.84 (15.63)	33.31 (19.53)	21.56 (4.21)	22.04 (6.85)	24.36 (9.12)	23.47 (8.82)	24.07 (9.24)	24.24 (9.74)
P_2	Min	35.89	35.89	36.26	35.89	35.89	35.89	35.89	35.89	35.89
	μ ($\pm\sigma$)	45.83 (28.53)	41.90 (20.98)	42.59 (9.39)	37.34 (1.08)	37.22 (1.00)	37.53 (1.52)	36.70 (0.81)	36.70 (0.93)	38.10 (8.22)
P_3	Min	57.92	57.75	58.26	58.25	58.10	57.94	57.92	57.92	57.92
	μ ($\pm\sigma$)	80.75 (24.00)	82.69 (25.11)	87.98 (29.78)	67.80 (14.35)	70.39 (17.46)	68.95 (15.65)	68.16 (16.38)	70.93 (22.18)	65.74 (14.79)
P_4	Min	21.10	21.37	21.10	21.10	21.10	21.10	21.10	21.10	21.05
	μ ($\pm\sigma$)	38.47 (20.23)	47.81 (30.48)	49.03 (29.14)	26.94 (12.66)	27.84 (13.73)	31.43 (15.61)	32.31 (15.99)	29.86 (14.89)	27.38 (13.18)
P_5	Min	24.72	1.97	2.02	1.97	1.97	1.97	1.97	1.97	1.97
	μ ($\pm\sigma$)	40.32 (17.75)	6.91 (11.71)	13.83 (16.72)	6.16 (12.19)	8.78 (13.26)	3.37 (4.21)	4.03 (6.91)	6.82 (12.06)	5.83 (10.06)
P_6	Min	24.72	24.76	24.76	23.53	24.59	24.11	24.16	24.25	24.04
	μ ($\pm\sigma$)	40.32 (17.75)	49.13 (23.60)	50.67 (21.71)	30.65 (10.73)	34.89 (14.50)	35.65 (13.88)	36.78 (15.94)	35.57 (15.93)	34.97 (14.29)
P_7	Min	8.88	9.10	9.10	8.79	8.83	8.79	8.79	8.79	8.72
	μ ($\pm\sigma$)	29.35 (28.09)	29.46 (27.20)	21.47 (15.41)	17.59 (14.43)	17.67 (17.64)	19.06 (18.73)	20.72 (20.78)	19.95 (19.03)	17.89 (17.53)
P_8	Min	5.86	5.86	5.96	5.86	5.86	5.55	5.55	5.81	5.86
	μ ($\pm\sigma$)	19.53 (20.18)	27.33 (27.34)	25.26 (22.00)	7.67 (6.96)	16.81 (17.95)	10.59 (17.24)	17.35 (19.16)	17.90 (18.19)	12.89 (15.11)
$P_1 \cdots P_8$	$\widehat{\mu}$ ($\pm\widehat{\sigma}$)	42.55 (16.63)	*39.38* (20.73)	40.52 (21.77)	*26.96* (18.41)	29.46 (17.85)	28.87 (18.82)	29.94 (17.73)	30.22 (17.93)	**28.38** (17.36)
	Sign.	–	–	–	=	–	–	–	–	–

MA based on SS with a deterministic application of LS

		Powell			Solis			XLS		
		25	50	100	25	50	100	25	50	100
P_1	Min	20.01	20.01	20.01	19.76	20.01	20.01	19.76	20.01	20.01
	μ ($\pm\sigma$)	28.20 (12.48)	30.21 (12.70)	33.45 (15.01)	21.35 (5.69)	21.51 (6.01)	24.52 (10.68)	23.40 (8.62)	20.99 (4.94)	21.00 (5.01)
P_2	Min	35.89	35.89	36.15	35.89	35.89	35.89	35.89	35.89	35.89
	μ ($\pm\sigma$)	42.65 (20.57)	44.32 (21.26)	49.49 (27.30)	37.74 (3.42)	37.05 (0.71)	37.10 (0.66)	36.36 (0.71)	36.44 (0.69)	36.69 (0.83)
P_3	Min	58.10	59.40	57.92	57.60	59.20	58.94	57.75	57.75	57.92
	μ ($\pm\sigma$)	77.27 (22.99)	84.88 (25.78)	78.90 (25.11)	72.36 (19.43)	70.17 (16.85)	66.54 (9.48)	64.20 (14.31)	61.70 (9.28)	64.55 (14.00)
P_4	Min	21.10	21.10	21.37	21.10	21.37	21.05	21.05	21.05	21.10
	μ ($\pm\sigma$)	40.51 (17.55)	46.55 (27.47)	55.05 (36.10)	24.86 (8.77)	26.55 (10.76)	28.26 (13.09)	26.52 (11.86)	27.50 (12.49)	21.46 (0.97)
P_5	Min	1.98	2.27	2.17	1.98	1.98	2.02	1.97	1.89	1.89
	μ ($\pm\sigma$)	11.90 (16.19)	12.23 (14.12)	17.02 (17.61)	2.79 (1.39)	4.28 (6.57)	5.27 (8.31)	3.53 (5.43)	2.78 (3.91)	3.19 (4.45)
P_6	Min	24.28	24.93	25.34	24.63	24.53	24.25	24.16	24.04	24.04
	μ ($\pm\sigma$)	43.99 (15.32)	47.31 (23.45)	54.54 (17.89)	32.72 (11.99)	33.83 (13.01)	34.57 (13.44)	30.27 (10.83)	31.25 (11.55)	27.64 (8.01)
P_7	Min	9.07	8.79	9.37	8.83	9.45	9.10	8.77	8.79	8.77
	μ ($\pm\sigma$)	22.15 (19.69)	33.78 (22.17)	36.82 (23.56)	14.75 (12.96)	21.08 (21.80)	20.87 (18.85)	10.68 (8.56)	15.18 (18.31)	16.68 (20.23)
P_8	Min	5.86	6.02	5.86	5.93	5.93	5.86	5.55	5.81	5.55
	μ ($\pm\sigma$)	27.69 (20.74)	34.30 (26.53)	35.84 (27.54)	7.95 (8.07)	13.14 (15.34)	12.86 (17.45)	10.19 (13.13)	9.23 (10.41)	10.37 (12.28)
$P_1 \cdots P_8$	$\widehat{\mu}$ ($\pm\widehat{\sigma}$)	*36.80* (18.47)	41.70 (19.51)	45.14 (17.42)	*26.81* (20.44)	28.45 (18.60)	28.75 (17.38)	25.64 (17.96)	25.63 (17.23)	**25.20** (17.66)
	Sign.	–	–	–	=	–	–	=	=	•

Bold values remark the memetic-based RIR method based on SS with the best performance when considering both the probabilistic and the deterministic application of LS

currently adopted sequential hybridization one. Nevertheless, taking into account the conclusion drawn for the first goal, improved RIR methods could be achieved by considering new advanced memetic designs based on the adaptation of parameters and operators involved in the evolutionary procedure (Ong et al. 2006).

With this work we consider the first stage of the mentioned research projects on the craniofacial identification problem is properly solved. Nevertheless, althought it is not a mandatory task now, we plan to tackle a different and more challenging RIR approach, called *multiview*, which could provide more accurate results at the expense of considering very demanding objective functions. Such a pitfall could be tackled by new memetic proposals facing computationally expensive optimization problems (Zhou et al. 2007). We are now involved in the second stage. We aim to design automatic, soft-computing based procedures to assist the forensic expert in the whole identification process.

Acknowledgments We want to acknowledge all the team of the Physical Anthropology Lab at the University of Granada (headed by Dr. Botella and Dr. Alemán) for their support during the data acquisition and validation processes. Besides, we would also like to thank Dr. Francisco Herrera and Dr. Daniel Molina for their useful suggestions regarding to non-parametric statistical tests. Especially, the authors would like to thank the anonymous referees as well as the guest editors for their valuable comments that allowed us to highly improve the paper quality.

Appendix

For a deeper understanding of the experimental study carried out in this work, Tables 8, 9, 10 and 11 show the individual results reported by the RIR methods based on both the sequential hybridization and the memetic approaches facing the eight designed RIR instances of our real-world problem: 3D reconstruction of forensic objects, human skulls in our case.

References

Bäck T, Fogel DB, Michalewicz Z (1997) Handbook of Evolutionary Computation. IOP Publishing Ltd/Oxford University Press, Bristol/Oxford

Ballerini L, Cordon O, Damas S, Santamaria J, Aleman I, Botella M (2007) Craniofacial superimposition in forensic identification using genetic algorithms. In: IEEE International Workshop on Computational Forensics (IWCF 2007), Manchester, pp 429–434

Besl PJ, McKay ND (1992) A method for registration of 3D shapes. IEEE Trans Pattern Anal Mach Intell 14:239–256

Beyer HG, Deb K (2001) On self-adaptive features in real-parameter evolutionary algorithms. IEEE Trans Evol Comput 5:250–270

Cordón O, Damas S, Martí R, Santamaría J (2008) Scatter search for the 3D point matching problem in image registration. INFORMS J Comput 20(1):55–68. doi:10.1287/ijoc.1060.0216

Cordón O, Damas S, Santamaría J (2006a) A fast and accurate approach for 3D image registration using the scatter search evolutionary algorithm. Pattern Recognit Lett 27(11):1191–1200

Cordón O, Damas S, Santamaría J (2006b) Feature-based image registration by means of the CHC evolutionary algorithm. Image Vis Comput 22:525–533

Cordón O, Damas S, Santamaría J (2007) A practical review on the applicability of different EAs to 3D feature-based registration. In: Cagnoni S, Lutton E, Olague G (eds) Genetic and evolutionary computation in image processing and computer vision. EURASIP Book Series on SP&C, pp 247–269

Costa D, Hertz A, Dubuis O (1995) Embedding of a sequential algorithm within an evolutionary algorithm for coloring problems in graphs. J Heuristics 1:105–128

De Falco I, Della Cioppa A, Maisto D, Tarantino E (2008) Differential Evolution as a viable tool for satellite image registration. Appl Soft Comput (in press)

Deb K, Joshi D (2002) A computationally efficient evolutionary algorithm for real-parameter optimization. Evol Comput 10(4):371–395

Dru F, Wachowiak MP, Peters TM (2006) An ITK framework for deterministic global optimization for medical image registration. In: Reinhardt JM, Pluim JPW (eds) SPIE, medical imaging 2006: image processing, pp 1–12

Eshelman LJ (1991) The CHC adaptive search algorithm: how to safe search when engaging in non traditional genetic recombination. In: Rawlins GJE (ed) Foundations of genetic algorithms 1. Morgan Kaufmann, San Mateo, EEUU pp 265–283

Eshelman LJ (1993) Real-coded genetic algorithms and interval schemata. In: Whitley LD (ed) Foundations of Genetic Algorithms 2. Morgan Kaufmann, San Mateo, EEUU pp 187–202

Fitzpatrick J, Grefenstette J, Gucht D (1984) Image registration by genetic search. In: IEEE Southeast conference. EEUU, Louisville, pp 460–464

Glover F (1977) Heuristic for integer programming using surrogate constraints. Decision Sci 8:156–166

Hart WE (1994) Adaptive global optimization with local search. PhD Thesis, University of California, San Diego

Herrera F, Lozano M, Molina D (2005) Continuous scatter search: an analysis of the integration of some combination methods and improvement strategies. Eur J Oper Res 169(2):450–476

Ikeuchi K, Sato Y (2001) Modeling from Reality. Kluwer,

Iscan M (1993) Introduction to techniques for photographic comparison. In: Iscan M, Helmer R (eds) Forensic analysis of the skull: craniofacial analysis, reconstruction, and identification. Wiley Liss, New York pp 57–70

Ishibuchi H, Yoshida T, Murata T (2003) Balance between genetic search and local search in memetic algorithms for multiobjective permutation flow shop scheduling. IEEE Trans Evol Comput 7(2):204–223

Jenkinson M, Smith S (2001) A global optimisation method for robust affine registration of brain images. Med Image Anal 5(2):143–156

Krasnogor N, Smith J (2000) A memetic algorithm with self-adaptive local search: Tsp as a case study. In: Genetic and evolutionary computation conference (GECCO'05), pp 987–994

Krasnogor N, Smith J (2005) A tutorial for competent memetic algorithms: model, taxonomy and design issues. IEEE Trans Evol Comput 9(5):474–488

Laguna M, Martí R (2003) Scatter search: methodology and implementations in C. Kluwer, Boston

Lehmann E (1975) Nonparametric statistical methods based on ranks. McGraw-Hill, New York

Lozano M, Herrera F, Krasnogor N, Molina D (2004) Real-coded memetic algorithms with crossover hill-climbing. Evol Comput 12(3):273–302

Maes F, Vandermeulen D, Suetens P (1999) Comparative evaluation of multiresolution optimization strategies for image registration by maximization of mutual information. Med Image Anal 3(4):373–386

Merz P, Freisleben B (1999) A comparison of memetic algorithms, tabu search, and ant colonies for the quadratic assignment problem. In: Angeline PJ, Michalewicz Z, Schoenauer M, Yao X, Zalzala A (eds) Proceedings of the congress on evolutionary computation, vol 3. Mayflower Hotel, Washington DC, IEEE Press, Piscataway, pp 2063–2070

Moscato P (1989) On evolution, search, optimization, genetic algorithms and martial arts: towards memeticalgorithms. Report 826, Caltech Concurrent Computation Program, Pasadena

Noman N, Iba H (2005) Enhancing differential evolution performance with local search for high dimensional function optimization. In: Genetic and evolutionary computation conference (GECCO'05), ACM, New York, pp 967–974

Ong YS, Lim M, Zhu N, Wong K (2006) Classification of adaptive memetic algorithms: a comparative study. IEEE Trans Syst Man Cybern B 36(1):141–152

Powell M (1964) An efficient method for finding the minimum of a function of several variables without calculating derivatives. Comput J 7:155–162

Press WH, Teukolsky SA, Vetterling WT, Flannery BP (1999) Numerical recipes in C: the art of scientific computing. Cambridge University Press, Cambridge

Price K (1999) An introduction to differential evolution. In: Corne D, Dorigo M, Glover F (eds) New ideas in optimization. McGraw-Hill, Cambridge pp 79–108

Salomon M, Perrin G-R, Heitz F (2001) Differential evolution for medical image registration. In: Arabnia H (ed) International conference on artificial intelligence IC-AI'2001, vol 2. CSREA Press, Las Vegas, pp 123–129

Santamaría J, Cordón O, Damas S, Alemán I, Botella M (2007) A Scatter Search-based technique for pair-wise 3D range image registration in forensic anthropology. Soft Comput 11:819–828

Satoh MYH, Kobayashi S (1996) Minimal generation Gap model for GAs considering both exploration and exploitation. In: Methodologies for the conception. Design and Application of Intelligent Systems (IIZUKA'96), pp 494–497

Shoemake K (1985) Animating rotation with quaternion curves. In: ACM SIGGRAPH. San Francisco, July 22–26, pp 245–254

Solis FJ, Wets RJB (1981) Minimization by random search techniques. Math Oper Res 6:19–30

Storn R (1997) Differential evolution—a simple and efficient heuristic for global optimization over continuous spaces. J Global Optim 11:341–359

Tang J, Lim M, Ong YS (2007) Diversity-adaptive parallel memetic algorithm for solving large scale combinatorial optimization problems. Soft Comput 11(9):873–888

Telenczuk B, Ledesma MJ, Velazquez JA, Sorzano COS, Carazo JM, Santos A (2006) Molecular image registration using mutual information and differential evolution optimization. In: IEEE international symposium on biomedical imaging: macro to nano, pp 844–847

Whitley D, Garrett D, Watson JP (2003) Quad search and hybrid genetic algorithms. In: Genetic and evolutionary computation conference (GECCO'03), ACM, New York, pp 1469–1480

Wolpert DH, Macready WG (1996) No free lunch theorems for search. Technical Report SFI-TR-95-02-010, The Santa Fe Insititute

Xu X, Dony RD (2004) Differential evolution with powell's direction set method in medical image registration. In: IEEE international symposium on biomedical imaging: macro to nano, pp 732–735

Yamany SM, Ahmed MN, Farag AA (1999) A new genetic-based technique for matching 3D curves and surfaces. Pattern Recognit 32:1817–1820

Yao J, Goh KL (2006) A refined algorithm for multisensor image registration based on pixel migration. IEEE Trans Image Process 15(7):1839–1847

Yoshizawa S, Belyaev A, Seidel HP (2005) Fast and robust detection of crest lines on meshes. In: SPM '05: proceedings of the 2005 ACM symposium on solid and physical modeling. EEUU, ACM Press, New York, pp 227–232

Zhang Z (1994) Iterative point matching for registration of free-form curves and surfaces. Int J Comput Vis 13(2):119–152

Zhou Z, Ong YS, Lim M, Lee B (2007) Memetic algorithm using multi-surrogates for computationally expensive optimization problems. Soft Comput 11(10):957–971

Zhu YM, Cochoff SM (2002) Influence of implementation parameters on registration of MR and SPECT brain images by maximization of mutual information. J Nuclear Med 43(2):160–166

Zhu Z, Ong YS, Dash M (2007) Wrapper-filter feature selection algorithm using a memetic framework. IEEE Trans Syst Man Cybern B 37(1):70–76

Zitová B, Flusser J (2003) Image registration methods: a survey. Image Vis Comput 21:977–1000